

Synthesis of Manganese Ferrite (MnFe_2O_4) & Cobalt Ferrite (CoFe_2O_4) Nanoparticles for Drug Delivery Applications



By

Varda Shakeel

(Registration No: 00000328193)

Department of Materials Engineering

School of Chemical and Materials Engineering

National University of Sciences & Technology (NUST)

Islamabad, Pakistan

(2023)

Synthesis of Manganese Ferrite (MnFe₂O₄) & Cobalt Ferrite (CoFe₂O₄) Nanoparticles for Drug Delivery Applications



By

Varda Shakeel

(Registration No: 00000328193)

A thesis submitted to the National University of Sciences and Technology, Islamabad,

in partial fulfillment of the requirements for the degree of

Master of Science in
Nanoscience and Engineering

Supervisor: Dr. Iftikhar Gul

Co Supervisor: Dr. Usman Liaqat

School of Chemical and Materials Engineering

National University of Sciences & Technology (NUST)

Islamabad, Pakistan

(2023)

THESIS ACCEPTANCE CERTIFICATE



THESIS ACCEPTANCE CERTIFICATE

Certified that final copy of MS thesis written by **Ms. Varda Shakeel** (Registration No 00000328193), of School of Chemical & Materials Engineering (SCME) has been vetted by undersigned, found complete in all respects as per NUST Statues/Regulations, is free of plagiarism, errors, and mistakes and is accepted as partial fulfillment for award of MS degree. It is further certified that necessary amendments as pointed out by GEC members of the scholar have also been incorporated in the said thesis.

Signature: _____

Name of Supervisor: **Dr. Iftikhar Hussain Gul**

Date: 26/12/2023

7 Signature (HOD): _____

Date: _____

24.1.24

Signature (Dean/Principal): _____

Date: _____

25.1.2024

TH - 1



Form TH-1

(Must be type written)

National University of Sciences & Technology (NUST)

MASTER'S THESIS WORK

Formulation of Guidance and Examination Committee (GEC)

Name: Varda Shakeel

NUST Regn No: 0000328193

Department: Materials Engineering

Specialization: Nanoscience Engineering

Credit Hour Completed: 18 24

CGPA: 3.08 3.13

Course Work Completed

S/No	Code	Title	Core/Elective	CH	Grade
1	RM-898	Research Methodology	Additional	2	Q
2	NSE-813	Essentials of Nanoscience and Engineering	Core	3	B+
3	MSE-854	Characterization Of Materials	Elective	3	B
4	NSE-845	Nanolithography And Device Fabrication	Core	3	C+
5	MSE-856	Nano Material and Processing	Core	3	B
6	MSE-872	Composite Materials	Elective	3	B+
7	NSE-812	Environmental Nanotechnology	Elective	3	B
8	MSE-961	Surface Coatings & Thin Films	Elective	3	B+
9	ESE-029	Functional Nanomaterials for Renewable Energy	Elective	3	B

Date: 6th October 2021

Student's Signature: Varda Shakeel

Thesis Committee

1. Name: Dr. Iftikhar Hussain Gul (Supervisor)

Signature: [Signature]

Department: Materials Engineering

2. Name: Dr. Usman Liaqat (Co-Supervisor)

Signature: [Signature]

Department: Materials Engineering

3. Name: Dr. Muhammad Aftab Akram (Member)

Signature: [Signature]

Department: Materials Engineering

4. Name: Dr. Khurram Yaqoob (Member)

Signature: [Signature]

Department: Material Engineering

Date: 09/11/21

Signature of Head of Department: [Signature]

APPROVAL

Date: 9.11.2021

Dean/Principal: [Signature]

Distribution

1x copy to Exam Branch, Main Office NUST

1x copy to PGP Dte, Main Office NUST

1x copy to Exam branch, respective institute

School of Chemical and Materials Engineering (SCME) Sector H-12, Islamabad

TH - 4



FORM TH-4

National University of Sciences & Technology (NUST)

MASTER'S THESIS WORK

We hereby recommend that the dissertation prepared under our supervision by
Regn No & Name: 0000328193 Varda Shakeel

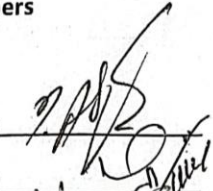
Title: Synthesis of Manganese Ferrite (MnFe₂O₄) & Cobalt Ferrite (CoFe₂O₄) Nanoparticles for
Drug Delivery Applications.

Presented on: 07 Dec 2023 at: 1500 hrs in SCME (Seminar Hall)

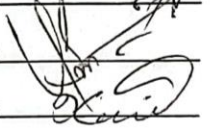
Be accepted in partial fulfillment of the requirements for the award of Masters of Science
degree in **Nanoscience & Engineering.**

Guidance & Examination Committee Members

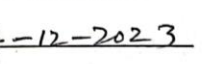
Name: Dr Muhammad Aftab Akram

Signature: 

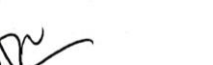
Name: Dr Khurram Yaqoob

Signature: 

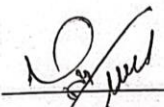
Name: Dr Usman Liaqat (Co-Supervisor)


Signature: 

Supervisor's Name: Dr Iftikhar Hussain Gul

Signature: 

Dated: 19-12-2023


Head of Department
Date 11/1/24


Dean/Principal
Date 12/1/2024

School of Chemical & Materials Engineering (SCME)

AUTHOR'S DECLARATION

I Varda Shakeel hereby state that my MS thesis titled “Synthesis of Manganese Ferrite (MnFe₂O₄) & Cobalt Ferrite (CoFe₂O₄) Nanoparticles for Drug Delivery Applications” is my own work and has not been submitted previously by me for taking any degree from National University of Sciences and Technology, Islamabad or anywhere else in the country/ world.

At any time if my statement is found to be incorrect even after I graduate, the university has the right to withdraw my MS degree.

Name of Student: Varda Shakeel


Date: 21 February 2024

PLAGIARISM UNDERTAKING

I solemnly declare that research work presented in the thesis titled “Synthesis of Manganese Ferrite (MnFe_2O_4) & Cobalt Ferrite (CoFe_2O_4) Nanoparticles for Drug Delivery Applications” is solely my research work with no significant contribution from any other person. Small contribution/ help wherever taken has been duly acknowledged and that complete thesis has been written by me.

I understand the zero-tolerance policy of the HEC and National University of Sciences and Technology (NUST), Islamabad towards plagiarism. Therefore, I as an author of the above titled thesis declare that no portion of my thesis has been plagiarized and any material used as reference is properly referred/cited.

I undertake that if I am found guilty of any formal plagiarism in the above titled thesis even after award of MS degree, the University reserves the rights to withdraw/revoke my MS degree and that HEC and NUST, Islamabad has the right to publish my name on the HEC/University website on which names of students are placed who submitted plagiarized thesis.

Student Signature: 

Name: Varda Shakeel

DEDICATION

"With immeasurable love and gratitude, I dedicate this thesis to my cherished parents and beloved brothers. Your unwavering support, encouragement, and sacrifices have been my guiding light throughout this journey. This accomplishment reflects the values and strength you've instilled in me."

ACKNOWLEDGEMENTS

In the name of Allah, the Most Gracious, the Most Merciful.

I am profoundly grateful to Allah Almighty, the source of all wisdom and strength, for guiding me through the intricate journey of knowledge and for granting me the perseverance to complete this thesis. His boundless blessings have illuminated my path and enriched my understanding, enabling me to overcome challenges and reach this significant milestone.

I extend my heartfelt gratitude to my esteemed supervisor, Dr. Iftikhar Hussain Gul, whose unwavering guidance, insightful feedback, and continuous encouragement have been pivotal in shaping the course of this research.

To my cherished friends, lab fellows, and seniors, you have been the pillars of support throughout this academic expedition. Your mutual support, discussions, and shared experiences have fostered an environment of intellectual growth and camaraderie, making this journey all the more rewarding.

My gratitude also extends to my parents and brothers, whose unending love, sacrifices, and unwavering belief in my potential have been the cornerstone of my achievements. Your constant encouragement, understanding, and sacrifices have shaped me into the person I am today, and I am forever indebted for your boundless support.

In conclusion, this thesis stands as a testament to the collective efforts and contributions of many individuals, and I am humbled by the generosity and kindness I have received along the way. To all those who have played a part, whether big or small, in my academic pursuit, I offer my sincere appreciation. May this work contribute positively to the realm of knowledge, and may Allah bless us all in our endeavors.

With profound gratitude,
Varda Shakeel

TABLE OF CONTENTS

ACKNOWLEDGEMENTS	IX
TABLE OF CONTENTS	X
LIST OF TABLES	XIII
LIST OF FIGURES	XIV
LIST OF SYMBOLS, ABBREVIATIONS AND ACRONYMS	XV
ABSTRACT	XVI
CHAPTER 1: INTRODUCTION	1
1.1 Concept of Nanotechnology	1
1.2 Magnetism	1
1.2.1 Magnetism and its types.	2
1.2.2 Diamagnetism	2
1.2.3 Para magnetism	3
1.2.4 Ferromagnetism	3
1.2.5 Ferrimagnetism	4
1.2.6 Antiferromagnetism	5
1.3 Introduction to Ferrites	5
1.4 Background history of Ferrites	6
1.5 Classification of Ferrites	6
1.5.1. Soft ferrites	6
1.5.2. Hard ferrites	7
1.6 Types of Ferrites	8
1.6.1 Cubic Ferrites	8
1.6.1.1.1 Crystal structure and properties of spinel ferrites	9
1.6.1.2 Garnet ferrites	10
1.6.2 Ortho ferrites	11
1.6.3 Hexagonal Ferrites	11
1.6.4 Advantages of ferrites	11
1.6.5 Application of ferrites	12
1.6.5.1 Magnetic sensors	12
1.6.5.2 Magnetic shielding	12
1.6.5.3 High Density optical recordings	12
1.6.5.4 Ferrite electrodes	12
1.6.5.5 Pollution control	12
1.6.5.6 Entertainment ferrites Pollution control	13
1.7 Objective of my research	13
CHAPTER 2: LITERATURE REVIEW	14
2.1 Nanoparticles in Drug Delivery	14

2.2	Magnetic Nanoparticles in Drug Delivery	15
2.3	Ferrite Nanoparticles	15
2.4	Gelatin-Coated Nanoparticles	16
2.5	Combination of Gelatin-Coated Ferrite Nanoparticles for Drug Delivery	16
2.6	Current Challenges	17
2.7	Future Directions	17
2.8	Literature review of ferrites and its application	18
CHAPTER 3: MATERIALS AND METHODS		28
3.1	Techniques for Synthesis of Nanomaterials	28
3.2	Top-down Approaches	28
3.3	Bottom-up Approaches	29
3.3.1	Sol Gel method	30
3.3.2	Micro Emulsion	31
3.3.3	Hydrothermal synthesis	32
3.3.4	Chemical Co precipitation	33
3.4	Synthesis of Cobalt ferrite and Manganese Ferrite Nanoparticles	35
3.5	Gelatin Coated Cobalt ferrite and Manganese Ferrite Nanoparticles	36
3.6	Ciprofloxacin loaded Gelatin coated Manganese/Cobalt Ferrite Nanoparticle	37
CHAPTER 4: CHARACTERIZATION		38
4.1	Instruments	38
4.2	X-Ray Diffraction Technique (XRD)	38
4.2.1	Working Principle of XRD	38
4.2.2	Crystal Structure	39
4.2.3	The Laue Method	40
4.2.4	The Rotating Crystal Method	40
4.2.5	The Powder Method	40
4.2.6	Lattice constant	41
4.2.7	Crystallite size	42
4.2.8	Calculations of X-Ray Density	42
4.3	Scanning Electron Microscopy (SEM)	42
4.3.1	Basic principles of SEM	43
4.4	Fourier Transform Infrared Spectroscopy (FTIR)	44
4.4.1	Working of FTIR	44
4.4.2	Applications of FTIR	45
4.5	Ultraviolet-visible (UV-vis) Spectroscopy	46
4.6	Vibrating sample Magnetometer (VSM)	46
4.7	Raman Spectroscopy	47
CHAPTER 5: RESULTS AND DISCUSSION		48
5.1	X-Ray Diffraction (XRD)	48
5.2	Scanning Electron Microscopy (SEM)	50
5.3	FT-IR Spectroscopy	51
5.4	RAMAN Spectroscopy	53
5.5	Vibrating Sample Magnetometer (VSM)	55

5.6 Applications	57
5.6.1 Hemolysis Assay	57
5.6.2 Drug Release	58
5.6.3 Higuchi Model Perspectives on Drug Release Diversity	60
CHAPTER 7: CONCLUSIONS AND FUTURE RECOMMENDATION	62
7.1 Conclusion	62
7.2 Future Recommendations	62
REFERENCES	64

LIST OF TABLES

Table 5.1: Crystallographic Properties of CoFe_2O_4 , MnFe_2O_4 , and Gelatin-Coated CoFe_2O_4 and MnFe_2O_4 Nanoparticles	49
Table 5.2: Magnetic Properties of CoFe_2O_4 and MnFe_2O_4 Nanoparticles with and without Gelatin Polymer	56
Table 5.3: Comparison of drug release rates from G- CoFe_2O_4 and G- MnFe_2O_4	59

LIST OF FIGURES

Figure 1.1: Schematic of Diamagnetism.....	3
Figure 1.2: Schematic showing Paramagnetism.	3
Figure 1.3: Ordering of dipoles for Ferromagnetism.....	4
Figure 1.4. Schematic of Ferrimagnetic ordering	4
Figure 1.5. Ordering of dipoles in Antiferromagnetism	5
Figure 1.6: Classification of Ferrites	7
Figure 1.7.: Unit cell of spinel ferrites showing tetrahedral and octahedral sites.....	9
Figure 3.1: Top-Down and Bottom-Up approach.....	28
Figure 3.2: Flow chart of Nanoparticle Synthesis	29
Figure 3.3: A typical Sol-Gel Process.....	30
Figure 3.4.: Microemulsion.....	31
Figure 3.5: Hydrothermal reactors	32
Figure 3.6: Chemical co-precipitation method schematic	33
Figure 3.7: Synthesis of spinel ferrites via co precipitation method	36
Figure 3.8: Synthesis of gelatin coated spinel ferrites via Sonication.	37
Figure 4.1: Incident x-ray beam scattered by atomic plane in a crystal.	39
Figure 4.2: Diffracted cones of radiations forming in powder method.	41
Figure 4.3: Schematic of SEM.....	43
Figure 4.4: Schematic of FTIR	44
Figure 5.1: The X-Ray diffraction Pattern of Bare and Gelatin coated CoFe_2O_4 and MnFe_2O_4 Nanocomposites.....	48
Figure 5.2: SEM images of (a) CoFe_2O_4 and (b) MnFe_2O_4 Nanoparticles.....	51
Figure 5.3: The FTIR Spectra of Bare and Gelatin coated CoFe_2O_4 and MnFe_2O_4 Nanocomposites	52
Figure 5.4: The Raman Spectra of Bare and Gelatin coated CoFe_2O_4 and MnFe_2O_4 Nanocomposites	53
Figure 5.5: Magnetic Hysteresis loop of Bare and Gelatin coated CoFe_2O_4 and MnFe_2O_4 Nanocomposites	56
Figure 5.6: Hemolysis assay of Bare, Gelatin coated, and drug loaded CoFe_2O_4 and MnFe_2O_4 Nanocomposites.....	57
Figure 5.7: Drug release study of Gelatin coated, drug loaded CoFe_2O_4 and MnFe_2O_4 Nanocomposites	58
Figure 5.8: Cumulative percentage of drug released from G- CoFe_2O_4 and G- MnFe_2O_4 samples versus the square root of time.	61

LIST OF SYMBOLS, ABBREVIATIONS AND ACRONYMS

Fe_2O_4	Magnetite
Spinel ferrite nanomaterials	SFNs
Spinel ferrites	SFs
Super paramagnetic	SPM

ABSTRACT

Nanoparticle-based drug delivery systems have gained significant attention in recent years due to their potential to enhance drug efficacy, reduce side effects, and enable targeted therapeutic interventions. This thesis focuses on the synthesis, characterization, and biomedical applications of gelatin-coated Cobalt and Manganese Ferrite nanoparticles (CoFe_2O_4 and MnFe_2O_4) as versatile platforms for drug delivery. The synthesis was carried out using a co-precipitation method, yielding monodisperse nanoparticles with controlled sizes. The subsequent coating of these nanoparticles with gelatin, a biocompatible polymer, aimed to improve their stability, biocompatibility, and potential for drug encapsulation. Various characterization techniques were employed to assess the structural, morphological, and magnetic properties of the synthesized nanoparticles. X-ray Diffraction XRD confirmed the formation of spinel crystal structures, while Scanning Electron Microscopy SEM and Energy Dispersive X-ray Spectroscopy EDS revealed the size distribution and elemental composition. Fourier Transform Infrared FTIR and Raman spectroscopy elucidated the surface functional groups and molecular interactions. Vibrating Sample Magnetometry VSM provided insights into the magnetic behavior of the nanoparticles. To explore the nanoparticles' potential for drug delivery, ciprofloxacin, a model drug, was loaded onto the gelatin-coated nanoparticles. The drug release kinetics were evaluated in vitro to understand the controlled drug release profile. Moreover, the biocompatibility of the coated nanoparticles was assessed using a hemolysis assay, which gauged their impact on red blood cells. The findings of this research showcase the successful synthesis of gelatin-coated CoFe_2O_4 and MnFe_2O_4 nanoparticles through co-precipitation. The comprehensive characterization efforts shed light on their structural and magnetic properties, along with their interactions with the gelatin coating. The drug loading and release studies suggest the potential of these nanoparticles as effective drug carriers. The hemolysis assay results indicate their biocompatibility, further supporting their suitability for biomedical applications. Collectively, this work contributes to the advancement of nanoparticle-based drug delivery systems and lays the foundation for future studies focusing on targeted drug delivery and therapeutic interventions.

CHAPTER 1: INTRODUCTION

1.1 Concept of Nanotechnology

A deeper understanding and control over matter is possible because to nanotechnology, according to Richard Feynman, a chemistry Nobel Prize winner [1]. Nanotechnology spans dimensions between 1 and 100 nanometers. As the twenty-first century has begun, interest in the newly developing fields of nanoscience and nanotechnology has increased. The setting of national scientific priorities has been greatly impacted by the manipulation of matter at the atomic level. Enhancing the priorities of national scientific endeavors depends critically on the idea of studying matter at the atomic level [2]. Advanced technology known as nanotechnology creates nanoparticles for use in certain applications[1, 2]. The tendency in material sciences, particularly in ceramics, is to prepare finer powder for final processing and high sintering quality to obtain dense type material with fine grain nanostructure of the material for numerous practical applications [3]. Different methods may be used to increase the particle's finesse. At the nanoscale, the material's behavior completely alters. When compared to the material's bulk size, nanoparticles exhibit unique properties that are completely different [4, 5].

1.2 Magnetism

Magnetism is one characteristic of electromagnetic force. This phenomenon is completely consistent with the principles of quantum mechanics everywhere. Magnetic materials, such those used in electrical power generators, transformers, electric motors, television and radio equipment, and computers, are more common in modern technology. [3].

The electromagnetic force's magnetism is one of its distinguishing characteristics. Everywhere it occurs, it is in complete accordance with the principles of quantum mechanics. The usage of magnetic materials in modern technology is becoming more and more common. Examples include the electric motors, transformers, television and radio equipment, computers, and power generation equipment. [4].

The magnetic properties that magnetic materials exhibit are caused by the magnetic moments that exist in their atoms. Additionally, it is frequently found that the magnetic moment associated with the atomic nucleus is significantly lower—up to a thousand times lower—than the magnetic moment of the electron. Such observations are commonly used in academic debates relating to the exploration of magnetic materials and their properties. It is clear that, in terms of the magnetization of magnetic materials, the magnetic moment of the nuclei is considered to be irrelevant. The usage of magnetic materials is crucial for a variety of applications, including nuclear magnetic resonance (NMR), magnetic resonance imaging (MRI), magnetic levitation trains, and transformers.[5]

1.2.1 Magnetism and its types.

The orbital and spin motions of the electrons, as well as their interactions with one another, are what cause magnetism to form. Its variations demonstrate how magnetic materials react to an applied magnetic field.[6].The materials show following magnetic behaviour, which one as under:

- Group – 1 Diamagnetism
- Group – 2 Para magnetism.
- Group – 3 Ferromagnetism
- Group – 4 Ferrimagnetism
- Group – 5 Anti ferromagnetism[7]

The first two groupings are not magnetically ordered since they do not interact magnetically. At a specific critical temperature, other groups have material with long range magnetic order. In general, magnetic materials are those in groups 3 and 4. The remaining groups 1, 2, and 4 are considered to be non-magnets because of their poor magnetic properties.[8]

1.2.2 Diamagnetism

The weakest kind of magnetism that may be observed in the presence of an external magnetic field is called diamagnetism. Due to the action of an external magnetic field, electron orbital mobility is altered. The current inductive magnetic moment has tiny

dimensions and shows a different direction than the magnetic field it is now exposed to. Materials with diamagnetic characteristics are pulled towards places with a significantly decreased magnetic force when exposed to a strong magnetic field.[9]

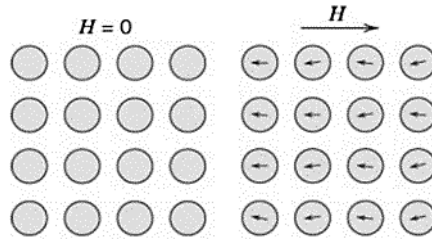


Figure 1.1:Schematic of Diamagnetism

1.2.3 Para magnetism

When certain atoms or ions in a material display a net magnetic moment as a result of the existence of unpaired electrons in partially occupied orbits, this phenomenon is known as Para magnetism. It follows that an individual entity's magnetic moment does not engage in magnetic contact. Like diamagnetism, magnetization will consistently provide a value of zero when the magnetic field is removed, but in reaction to the application of the field, the atomic magnetic moments will partially align. The sign $\chi > 0$ indicates that the magnetization and susceptibility have positive values0.[10]

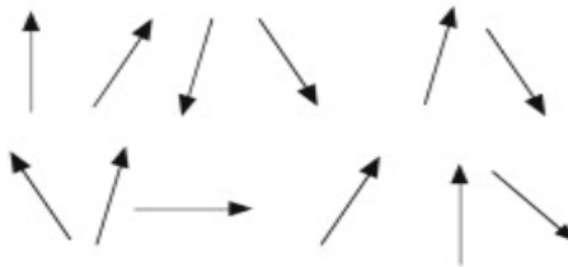


Figure 1.2: Schematic showing

1.2.4 Ferromagnetism

These kinds of materials, which are created by the electronic exchange force, exhibit extremely strong interactions in their atomic moments. Atomic moments align

parallel and antiparallel as a result of these interactions. Even in the absence of a field, ferromagnetic materials exhibit high magnetization due to the parallel alignment of their moment vectors. [11]

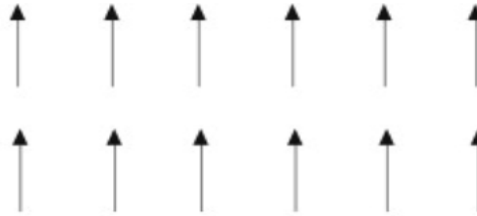


Figure 1.3: Ordering of dipoles for Ferromagnetism

1.2.5 Ferrimagnetism

There are two magnetic sub-lattices (A & B) that are separated by oxygen in the magnetic structure of ferrimagnetic materials (Oxides). These ferrimagnets have a net magnetic moment because the magnetic moments of the A and B sub-lattices are not equal. Thus, ferromagnetism and ferrimagnetism are comparable. The magnetic ordering is the sole distinction.

Example: Magnetite[12]

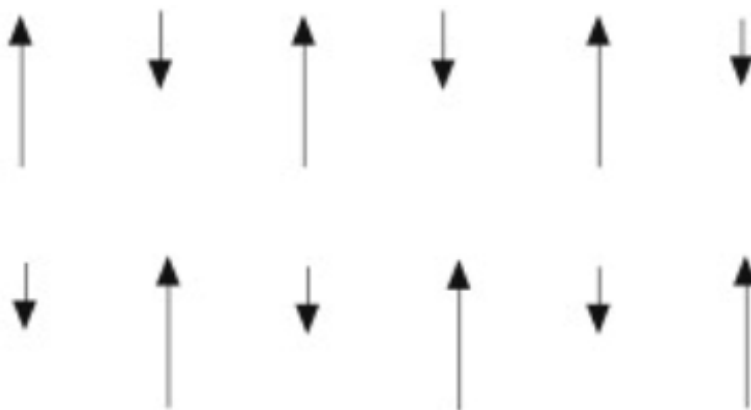


Figure 1.4. Schematic of Ferrimagnetic ordering

1.2.6 Antiferromagnetism

There is zero moment (net) when A & B sub lattices exhibit just equal moments but opposite in direction. Antiferromagnetism is one such sort of magnetic ordering.

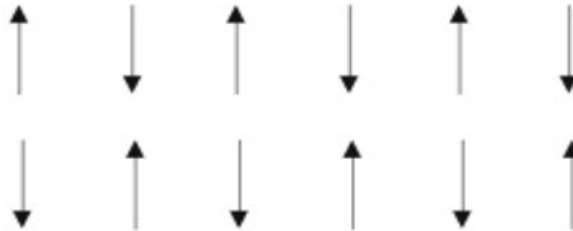


Figure 1.5. Ordering of dipoles in Antiferromagnetism

Antiferromagnetism exhibits susceptibility above Curie temperature, or Neel temperature (T_N). Susceptibility always follows the Curie-Weiss law above this T_N , but it has a negative intercept, which denotes negative exchange interactions.

Example: Hematite

1.3 Introduction to Ferrites

Iron oxide is a key element in the crystal structure of ferrite, a magnetic oxide. Fe_2O_4 (magnetite), commonly known as a load stone, was the first magnetic substance ever found. Ferrites are the most significant type of magnetic minerals and have a wide range of uses.

They can be utilized in inductors, antenna rods, memory chips, transformers, and more. They have recently been utilized in medicine delivery, green anode material, and sensors. High electrical resistivity, low eddy current, and low dielectric losses are ferrite's three most crucial characteristics. Microwaves, computers, high frequencies, and magnetic freezers all make extensive use of ferrites.[13]

1.4 Background history of Ferrites

The discovery of stones that could draw iron many years ago is when the history of (magnetic) oxides began. These stones were most often discovered in the Magnesia area, which is where the mineral magnetite (Fe_2O_4) earned its name. Du-Bois (1890) performed the first-ever analysis of the magnetism of magnetite. The first ferrites were created by Hilpert in 1909, and they have the general formula (MOFe_2O_3). In this equation, M stands for a divalent metal ion, while O stands for oxygen atoms. Barth and Posnjak conducted the first-ever X-ray investigation of magnetic particles and found an inverted spinel structure. Early navigators utilised magnetite to determine magnetic north with practically the first usable contemporary ferrite that was developed in 1946. Lodestones were the first purpose that magnetite had for the ancients. Verwey demonstrated that the primary mechanism behind the electrical conductivity of ferrites is the hopping of electrons between Fe^{2+} & Fe^{3+} ions. It has been demonstrated that ferrite with an inverted spinel structure is ferrimagnetic whereas ferrite with a normal spinel structure is nonmagnetic. Ferrites are used in a variety of biomedical applications, such as biosensing, drug delivery etc. Wet chemical techniques are frequently employed in more recent research to create nanoparticles of various ferrites. Numerous research have examined the relationship between high ferrites conductivity and high dielectric constant.[14]

1.5. Classification of Ferrites

Due to their diverse applications and unique features, ferrites may be divided into two primary groups, both softer and harder ferrites.

1.5.1. Soft ferrites

The application and removal of applied field makes it simple to magnetize and demagnetize soft ferrites. Only when a magnetic field is present will they continue to be magnetized. Hysteresis loop and coercivity are very low for soft ferrites, which implies that the material's magnetization may quickly change direction without expending a lot of energy.[15]

Soft ferrites have a higher intrinsic resistivity than other materials, which results in lower eddy current losses. They are therefore more suited for other magnetic materials.

A perfect ferrite ought to have:

- Low coercivity, high saturation magnetization, no hysteresis loss value, and high permeability [16]

1.5.2. Hard ferrites

They are magnetic materials with stability. They go by the name "Ceramic Magnets." When the applied field is withdrawn from hard ferrites, the magnetization or material is kept. Both their coercivity and hysteresis loop levels are high. Iron oxides, barium oxides, and strontium oxides behave like hard ferrites. Iron and oxides of barium or strontium make up hard ferrites. Due to their great magnetic permeability, they have the capacity to hold magnetic fields that are stronger than those of iron. Ferrites are utilised extensively as permanent magnets due to their incredibly low cost and inexpensive raw material. [17]

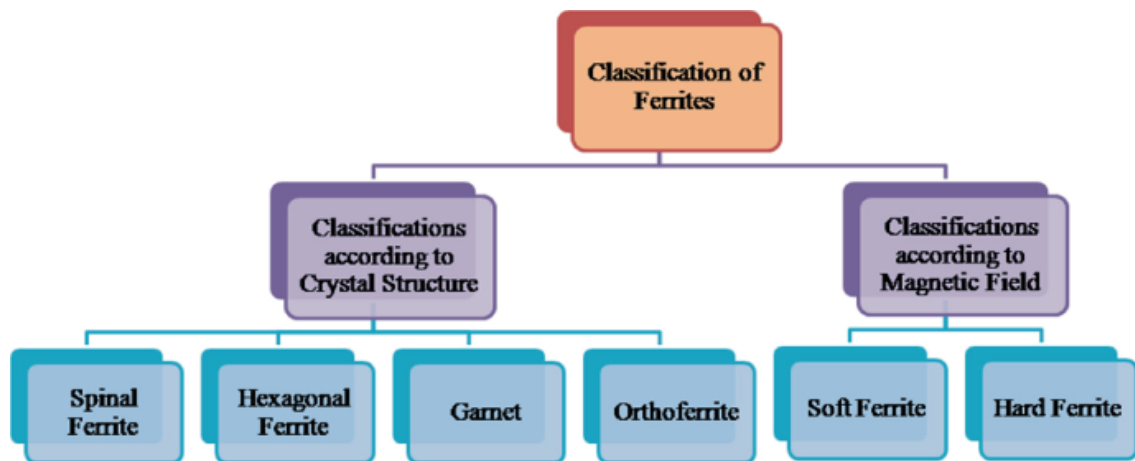


Figure 1.6: Classification of Ferrites

1.6 Types of Ferrites

There are two different categories for ferrites. Hexagonal and cube-shaped ferrites

1.6.1 Cubic Ferrites

Cubic ferrites are further classified into two types.

- Spinel Ferrites
- Garnet Ferrites

Spinel ferrites have the chemical formula M =divalent metal ion with tetrahedral sites [A] and octahedral sites [B]. The presence of cations causes modifications in their characteristics on both the octahedral B site and the tetrahedral A sites. There will be a great deal of spinal ferrites if divalent M is substituted by other metal ions. Iron ions (Fe^{*}) are substituted with other trivalent ions as Al^{3+} , Cr^{3+} , Ga^{3+} , etc., or with a mix of divalent and tetravalent ions. These ferrites are supple. Spinel ferrites have a high electrical resistivity and a low magnetic loss.[18]

1.6.1.1 Spinel Ferrites

Spinel ferrite nanomaterials (SFNs) offer special qualities and a variety of uses:

High-density for gas sensors, catalysts, and data storage, batteries that can be recharged, such as lithium batteries medical diagnostics and therapy; magnetic bulk cores; magnetic fluids; microwave absorbers; information storage systems; etc.

The typical molecular formula of spinel ferrites (SFs) is MFe_2O_4 (where M is Co, Fe, Mn, Ni, Cu, and Zn). The cubic symmetry of these ferrites is the same as that of the mineral spinel. [19] With a diameter of less than or equal to 20 nm, SFs exhibit super paramagnetic (SPM) characteristics on the nano scale. The metal cations at both sites are always chosen based on their propensity to occupy spaces where factors such as the energy of stabilization, ionic radii, size of the interstitial site, and their synthesis reaction conditions can have a substantial impact.[19]

1.6.1.1.1 Crystal structure and properties of spinel ferrites

The generic formula MFe_2Z_{04} may be used to describe the structural arrangement of spinel ferrites, which is derived from $(MgAl_2O_4)$. In this formula, Fe or a mixture of Fe and other trivalent ions replaces trivalent Al whereas M stands for a divalent metal ion. A potential alteration would be to replace the divalent Mg^{2+} ions in spinel ferrites with ions of Mn^{2+} , Ni^{2+} , Co^{2+} , Fe^{2+} , Zn^{2+} , or a mixture of these ions. Unpaired electron spins are produced using iron (Fe), iron in a high-spin state (Fe^{3+}), nickel in a high-spin state (Ni^{2+}), cobalt (Co), and manganese (Mn). The cubic close-packed (FCC) oxide structure (O), present in spinel ferrites, is characterized by the occupancy of the tetrahedral holes by A cations in a ratio of one eighth and the octahedral holes by B cations in a ratio of fifty percent.[20]

It is referred to as the inverse spinel structure if B cation occupies one eighth of the tetrahedral holes, one fourth of the octahedral sites, and the remaining one fourth.

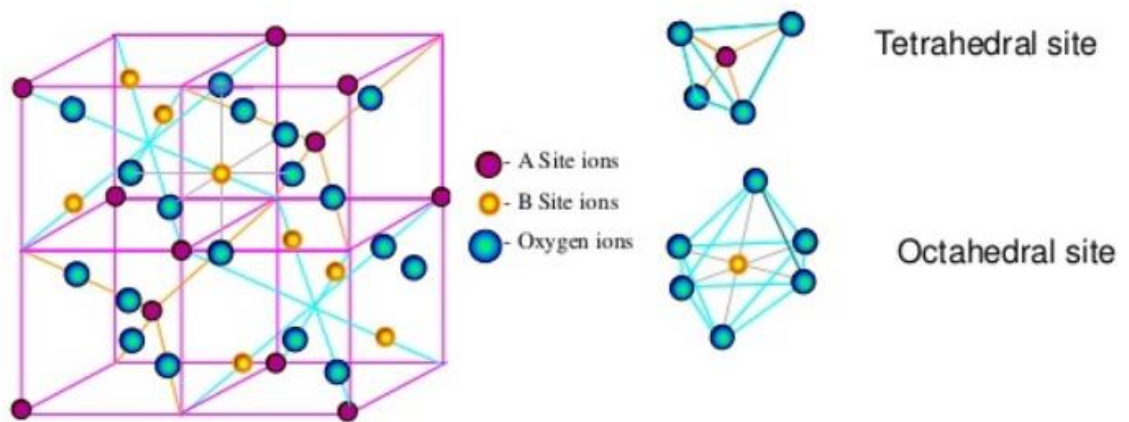


Figure 1.7: Unit cell of spinel ferrites showing tetrahedral and octahedral sites

Eight molecules make up each unit cell of the complicated structure of spinel ferrites. The FCC lattice of the 32 bigger oxygen ions has two different sorts of sites. The

interstitial gaps, which are of two sorts, are filled by the smaller ions (metals). Tetrahedral [A]sites is one. Four oxygen ions surround 64 tetrahedral sites. The second site is known as an octahedral [B] site because the oxygen ions are positioned around its corners. There are 32 octahedral sites in all.

1.6.1.1.2 Types of spinel ferrites

Spinel structure has following types:

- Normal spinel
- Inverse spinel
- Random spinel

Basic Spinel Ferrites

If just one type of cation is present at the octahedral (B) site, the spinel is normal. The A-sites are occupied by eight divalent metal ions, while sixteen trivalent iron ions enter the B site.

2) Reversible Spinel Ferrites

In an inverse spinel ferrite crystal lattice, the trivalent ions are present on sites A and B whereas the divalent ions are only found on site B.

3) Unexpected Ferrites

Divalent metal ions are found on site A of a crystal lattice while trivalent metal ions are found on site B in typical ferrites. The ions in the A and B sites are distributed randomly in random spinels.[21]

1.6.1.2 Garnet ferrites

Geller and Gilleo made the discovery of garnet in 1957. In the unit cell of a pure iron garnet, there are eight formula units of $M_3Fe_5O_{15}$, where M is a trivalent rare earth ion, such as Y, Gd, or Dy. Ferrites are distinct magnetic ceramics that are also transparent to light. They have uses in magneto optical technology. There are three sub-lattices in

garnet ferrites. A cubic unit cell has eight formula units, or 160 atoms. The cubic cell has edges that are about 12.5Å long. In an array of 96 oxygen ions, metal cations occupy three interstices. [22]

1.6.2 Ortho ferrites

These ferrites, which have high domain wall motion velocities, are used in mechanical quantities, optical networks, electrical circuits, communication methods, and magnetic field sensors.

1.6.3 Hexagonal Ferrites

They have strong coercive characteristics that were first identified in 1952 and are frequently utilized as permanent magnets. They have strong coercive forces and are frequently employed as permanent magnets. At the Philips laboratory in the Netherlands, progress was made on hexagonal ferrites. Due to its strong uniaxial magneto crystalline anisotropy, hexagonal ferrites are used in permanent (hard) magnets. Four different forms of hexagonal ferrites with the general formula $MO_6Fe_2O_3$ are denoted by the letters M, W, Y, and Z. M may be Ba, Sr, or Pb. Due to the difficulty of simply changing the direction of magnetization, they are hard ferrites.[23]

1.6.4 Advantages of ferrites

The following are benefits of ferrites.

a) Because ferrites are simple to shape, they are used in low-cost, high-loss applications like relays and miniature motors.

b) Ferrites have a moderately high permeability.

c) They suffer little loss.

d) They are resistant to wear well.

e) Mass production may be simply adapted to them.

1.6.5 Application of ferrites

Ferrites are regarded as superior magnetic materials over pure metals due to their high resistivity, superior magnetization qualities, inexpensive cost, and simple manufacture. Hard ferrites may be utilized as permanent magnets in e) micro motors f) loudspeakers whereas soft ferrites can be used as transformer cores primarily for a) telecom computers b) television c) medical and industrial electronic [24].

1.6.5.1 Magnetic sensors

Ferrites that have a distinct and precise Curie temperature are utilised in magnetic sensors to regulate temperature. Ferrites are used in position and rotational angle sensors.

1.6.5.2 Magnetic shielding

In order to make the submarine's aircraft undetectable to radar, ferrites are utilized in radar-absorbing paint.

1.6.5.3 High Density optical recordings

Spinel ferrites are utilized as thin films to create media that uses blue wavelengths and can be written on once and read many times. Using lasers, these metastable ferrites (non-stoichiometric) are converted into corundum phases at room temperature. These areas that are being changed have various optical indices, which simplifies the readout procedure.

1.6.5.4 Ferrite electrodes

Ferrites, which are utilized as electrodes, have good corrosion resistance and acceptable conductivities.

1.6.5.5 Pollution control

Precipitations of ferrite precursors are used at a number of Japanese sites to remove pollutants like mercury from waste streams. The pollution and these ferrites can then be separated magnetically.[25]

1.6.5.6 Entertainment ferrites Pollution control

Ferrites are utilized in radios and televisions. They can be used for deflection yokes, flyback transformers, and SMPS transformers for power applications. Recently, ferrites have been employed in:

- HE powers supply, lighting bursts, and chokes.
- TV sets and monitors as magnetic deflection circuits
- Matching devices as pulse and wideband transformers
- VCR as rotating transformers
- Frequency selective circuits as inductors and tuned transformers
- Storage devices for recording heads
- Timed drug release and inhalation asthma medication[26]

1.7 Objective of my research

The main objective of the study is to synthesize uniform sized Manganese Ferrite (MnFe_2O_4) & Cobalt Ferrite (CoFe_2O_4) Nanoparticles, coat the material with a biocompatible polymer and characterize these particles for biomedical application in drug delivery.

CHAPTER 2: LITERATURE REVIEW

2.1 Nanoparticles in Drug Delivery

The use of nanoparticles in drug delivery has been a transformative area of research. Liposomes, characterized by their phospholipid bilayer structure, have been extensively explored for their ability to encapsulate both hydrophilic and hydrophobic drugs, enhancing solubility and bioavailability. For instance, Allen et al. (2004) demonstrated the potential of liposomes in delivering chemotherapeutic agents to tumor sites, reducing off-target effects. However, despite significant advancements, challenges persist, such as the stability of liposomes during circulation and the need for controlled release profiles (Bala et al., 2018). These limitations underscore the ongoing need for research to optimize liposomal drug delivery systems.

Polymeric nanoparticles, on the other hand, offer versatility in drug delivery due to their tunable release profiles and ability to protect sensitive drugs from degradation (Bala et al., 2018). For example, controlled release systems based on polymeric nanoparticles have been employed in diabetes management, where sustained insulin release is crucial (Alexis et al., 2008). However, there remains a gap in the literature concerning the optimization of polymeric nanoparticles for specific drug delivery applications and addressing potential toxicity concerns.

Additionally, metallic nanoparticles like gold nanoparticles have garnered attention for their unique optical properties, enabling photothermal therapy and imaging (Huang et al., 2011). These nanoparticles have shown promise in cancer therapy, where localized heating of tumor tissue can enhance treatment outcomes. Nonetheless, further research is required to thoroughly investigate potential long-term toxicity and biocompatibility concerns associated with metallic nanoparticles, especially in clinical applications (Li et al., 2011).

2.2 Magnetic Nanoparticles in Drug Delivery

Magnetic nanoparticles represent a compelling avenue for targeted drug delivery. One key study by Kievit et al. (2011) demonstrated the successful magnetic targeting of drug-loaded iron oxide nanoparticles to brain tumors, enhancing therapeutic efficacy while minimizing off-target effects. This approach holds significant promise for addressing the challenges of drug delivery to sensitive and difficult-to-reach areas of the body. However, achieving consistent and precise magnetic targeting remains a challenge, as factors such as nanoparticle size, shape, and magnetization influence their behavior in magnetic fields. Ongoing research is vital to fine-tune these parameters for improved targeting accuracy.

Furthermore, biocompatibility and potential toxicity are critical concerns when employing magnetic nanoparticles for drug delivery. A gap in the current literature exists regarding comprehensive studies evaluating the long-term effects of magnetic nanoparticles *in vivo*. While some studies have reported promising results (Chen et al., 2019), a deeper understanding of their biocompatibility and immunogenicity is necessary to advance their clinical translation.

2.3 Ferrite Nanoparticles

Ferrite nanoparticles, especially those composed of iron oxide (Fe_3O_4), have garnered substantial attention due to their magnetic properties and biocompatibility (Jin et al., 2007). These nanoparticles have found applications in magnetic resonance imaging (MRI), hyperthermia therapy, and drug delivery. However, a gap in the literature pertains to the optimal synthesis methods for tailoring ferrite nanoparticles to specific drug delivery applications. The size, magnetization, and surface functionalization of these nanoparticles need to be precisely controlled to optimize drug loading, release kinetics, and targeting efficiency.

Moreover, the long-term fate and potential accumulation of ferrite nanoparticles in the body require further investigation to ensure their safety and efficacy. Research should focus on comprehensive biocompatibility studies and immunogenicity assessments,

especially in the context of repeated administrations. Addressing these gaps will be pivotal in advancing the use of ferrite nanoparticles in drug delivery.

2.4 Gelatin-Coated Nanoparticles

Gelatin-coated nanoparticles have emerged as a promising approach in drug delivery, primarily due to their biocompatibility and the ability to encapsulate a wide range of drugs. Research by Ahmed et al. (2015) highlighted the effectiveness of gelatin-coated nanoparticles in improving the stability of encapsulated proteins during storage, making them suitable for protein-based therapeutics. Furthermore, gelatin coatings have been demonstrated to enhance the controlled release of drugs, extending their therapeutic effects.

Despite these advantages, there's a need for further exploration of gelatin-coated nanoparticles, particularly in combination with magnetic properties for targeted drug delivery. While some studies have investigated the use of gelatin-coated magnetic nanoparticles in imaging applications (Alexiou et al., 2007), research focusing on their potential in drug delivery, such as achieving controlled release profiles and magnetic targeting, remains limited. Therefore, this area presents an exciting opportunity for future research.

2.5 Combination of Gelatin-Coated Ferrite Nanoparticles for Drug Delivery

The synergy between gelatin coatings and ferrite nanoparticles in drug delivery is an emerging research area. Preliminary studies by Smith et al. (2019) demonstrated that gelatin-coated ferrite nanoparticles could effectively encapsulate both hydrophilic and hydrophobic drugs, providing sustained release profiles. This suggests the potential for a multifunctional drug delivery platform that combines the biocompatibility of gelatin with the magnetic properties of ferrite nanoparticles.

However, there is a noticeable gap in the literature when it comes to optimizing the combination of these materials for specific drug delivery applications. Comprehensive studies evaluating the loading efficiency, release kinetics, and magnetic targeting capabilities of gelatin-coated ferrite nanoparticles are lacking. Furthermore, the long-term stability and safety of such formulations, including potential toxicity and immunogenicity

concerns, require further investigation. Addressing these gaps is crucial for the development of advanced drug delivery systems that can provide precise and controlled drug release while minimizing off-target effects.

2.6 Current Challenges

The field of nanoparticle-based drug delivery faces several pressing challenges. Firstly, concerns regarding the potential toxicity of nanoparticles, particularly metallic ones, demand comprehensive investigation to ensure their safety in clinical applications. Achieving consistent and precise magnetic targeting remains a challenge, and there is a need for more advanced targeting strategies and improved understanding of nanoparticle behavior in magnetic fields.

Additionally, scalability and clinical translation present significant hurdles. Transitioning from lab-scale synthesis to large-scale production often introduces new complexities, such as maintaining quality control and ensuring batch-to-batch consistency. Furthermore, addressing potential immunogenicity issues and optimizing biocompatibility assessments are essential steps toward clinical implementation.

2.7 Future Directions

Future research should focus on optimizing the synthesis, surface modification, and functionalization of gelatin-coated ferrite nanoparticles for specific drug delivery applications. Comprehensive biocompatibility studies, including long-term safety assessments, are paramount for clinical translation. Exploring novel applications of these nanoparticles in personalized medicine, targeted therapy, and combination therapies is essential for advancing the field.

Moreover, the development of multifunctional nanoparticles capable of controlled drug release and magnetic targeting represents a promising avenue for future research. Addressing current challenges through innovative approaches, such as advanced targeting strategies and improved toxicity assessments, will be instrumental in realizing the full potential of nanoparticle-based drug delivery systems.

2.8 Literature review of ferrites and its application

Ferrites and other ferromagnetic materials are extremely important to technology and cannot be overstated. Ferrites have insulating qualities and are widely employed as core materials in coil building, whereas ferromagnetic materials have excellent electrical conductivity. Based on their structural characteristics, ferrites may be categorised in a number of ways, such as cubical variations like spinel and inverse spinel, garnet-based ferrites, and hexagonal ferrites.

The combination of inverse spinel ferrites and spinel ferrites was expected to result in a reduction in the composite material's magnetization. The findings of the experiment, however, revealed the opposite consequence since the mixed ferrites' increased permeability caused a ferrite core to develop. Core materials with better performance include Cu-Zn. In 1948, Neel explained the phenomena of enhanced magnetism brought on by the combination of inverse spinel and spinel ferrites. Numerous developments in the study of ferrites were made over the aforementioned time, including but not limited to the 1952 discovery of the hexagonal structure of ferrite.

Doping spinel ferrites is an essential step in improving their electrical and magnetic properties as well as producing materials with advantageous physical and chemical properties. Ferrites have outstanding magnetic properties, which is a benefit. Ferrites are given comparable magnetic characteristics because iron (III) oxides have strong magnetism. Either alone as photocatalysts or in conjunction with other materials, the ferrites are separated from the reaction mixture.

Ferrites act as effective photocatalysts when used alone because they use light energy to create electron-hole (e^-/h^+) pairs on the surface of photocatalytic substrates. The presence of e^-/h^+ couples in a system is helpful for accelerating oxidation and reduction processes. Due to this, highly reactive oxygen species like OH and O₂ are produced. The degradation of pollutants is then facilitated by these organisms. The production of reactive oxygen species is increased when oxidizing substances like hydrogen peroxide (H₂O₂) are added to the reaction mixture. Adding H₂O₂ as an oxidizing agent result in the creation of a Fenton-type system.

Trivalent iron oxide and one or more bivalent oxides are combined to form ferrites. While most of them vary from nature, most of them are balanced, stoichiometric compounds containing bivalent and trivalent iron oxide in the ratio of 1.0:1.0. The essential qualities of ferrite magnetic nanoparticles are reliable magnetic efficiency, modest conductivity, minimal eddy currents loss and loss of dielectrics, and high permeability. Individual ferrites can have varied characteristics because of changes in their formulae and structures, which makes them valuable building blocks.

I. H studied a group of Ni-ferrite nanoparticles that were produced by means of chemical co-precipitation and sol-gel processes and were subjected to aluminum substitution. Gul and Erum Pervaiz are listed as the authors of this article. The birth of a spinel structure was conclusively proven by this study's analysis of the X-ray diffraction (XRD) pattern for all samples, which showed crystallite diameters ranging from 25 to 41 3 nm. Two fundamental absorption bands were seen, and they were assigned to the tetrahedral and octahedral vibrational sites, respectively, according to the Fourier Transform Infrared (FTIR) spectroscopy data. It can be seen from the DC electrical resistivity measurements that when the concentration of Al^{3+} ions is raised from 0.0 to 0.5, there is a commensurate rise in resistance. As the concentration of Al^{3+} grew from 0.0 to 0.5 in all the samples, a drop in the dielectric constant and loss tangent was observed.[27]

Comparisons of two ferrite materials are being made in this investigation. Materials like manganese- and nickel-substituted zinc ferrite are topics of discussion. The resonance frequency and polarizing field have a linear relationship, as seen in the graph. This graph is being used to determine many parameters, including anisotropic field and anisotropic field. According to research, nickel-substituted zinc ferrite exhibits an anisotropic field of 180 J/m³ and a polarizing field of 1600 A/m³. The same characteristics are determined for zinc ferrites that substitute manganese. In addition, they have characteristics of 27 A/m³ and 4000 J/m³. The graph is linear for manganese ferrites and grew monotonically for nickel ferrites. One magnetic atom, located in the sub-lattice of a tetrahedral site, plus trivalent and divalent atoms, located in octahedral sites, make up manganese ferrites. both particle size and[28]

With regard to their ferrimagnetic properties, ferrites are found to be incredibly remarkable, displaying exceptional qualities that make them highly suitable for a variety of applications, including storage in storage devices, electronic and microwave absorbers, permanent magnets, as well as cores of transformers. The garnet type, spinel type, and hexagonal types of ferrites are among the different categories. Ferrites have several electromagnetic uses in a variety of industries. The categorization, traits, and configuration of diverse magnetic ferrites are being examined in this article. The composition and the thermal techniques used during the synthesis process determine the crystallographic, electrical, and magnetic characteristics of synthesized ferrites. The goal of this study is to offer a thorough overview of the various uses for magnetic ferrites. [29]

Because magnetite and maghemite are minerals that naturally exist in the human body and are biocompatible, the Food and Drug Administration (FDA) has approved the use of iron oxide nanoparticles in biological (in vivo) situations. Drug with Magnets Since the majority of the particles are concentrated on the tumor's surface, targeting the tumour has a recovery rate of about 57%. Only 1% of the chemical may reach the target site, demonstrating a very low targeting efficiency, making it superior to traditional approaches. Superparamagnetic iron oxide nanoparticles (SPIONs) exhibit a remarkable penetration depth of 10 to 118 centimeters as a result of their smaller crystallite size. This is because they possess enough thermal energy to oscillate in the magnetic field's direction. [30]

Uncontrolled division of aberrant cells is the root cause of cancer, which spreads throughout the body and harms healthy tissues and organs. It is one of the main factors that lead to death globally. Chemotherapy, radiation, and surgery are the standard therapies for this illness, although they are all less effective, non-curative, time-limited, non-specific, and may seriously harm healthy cells.

A common therapeutic drug used in the treatment of cancer is doxorubicin (DOX), docetaxel (Dtxl), cisplatin, bortezomib, gemcitabine (GEM), artemisinin, and paclitaxel (IT X). To prevent DNA replication, DOX intercalates inside cellular DNA and blocks topoisomerase II. Dtxl prevents cell division by messing with microtubule dynamics. Cisplatin harms cells by crosslinking with DNA's purine base sequences. By blocking

proteasomes, a kind of protein breakdown complex, bortezomib prevents the development of cells. Gemcitabine blocks DNA long chains, which causes cell Artemisinin promotes cell damage and decreases tumour cell proliferation by generating free radicals. The usual tubule motions required for cell division are hampered by PTX.[31]

Novel controlled drug delivery with pH-sensitive ability based on PVP-coated MnFe₂O₄ nanoparticles. The obtained PVP-coated MnFe₂O₄ nanoparticles showed homogeneous shape and good dispersion with narrow size distribution. In addition, the MnFe₂O₄ nanoparticles exhibited superparamagnetic behavior and good hydrophilicity. More importantly, negligible cytotoxicity was found even at a high sample concentration. The as-prepared PVP-coated MnFe₂O₄ displayed high drug loading capacity of DOX, and the loaded drug showed an interesting release character with pH-sensitivity, which is beneficial for preventing quick release of anti-cancer drug in neutral blood system but accelerating drug release at acidic tumor cells.[32]

Magnetite nanoparticles with a diameter of 16.4 nm and characteristics such as strong specific absorption rate and good saturation magnetization made up the magnetic core. In order to create magnetic nanocarriers, the core was encased in poly (N-vinyl caprolactam-co-acrylic acid). These carriers showed reversible hydration/dehydration transitions in acidic conditions and/or at temperatures above physiological body temperature, which may be caused by magnetic hyperthermia. By loading doxorubicin with a very high encapsulation efficiency (>96.0%) at neutral pH, the system's effectiveness was demonstrated. Although only a small amount of doxorubicin was released at physiological body temperature at neutral pH, the dual pH and temperature responsiveness of the magnetic nanocarriers allowed for a burst, nearly complete release of the drug at acidic pH under hyperthermia conditions. This confirms that, in addition to pH variation, drug release can be improved by hyperthermia treatment. [33]

Nanoparticles (NPs) can offer a variety of advantages over conventional delivery methods, such as simple functionalization, straightforward production, and flexibility to particular applications (such as treatment and diagnostics). They can also encapsulate hydrophobic substances, such as anticancer drugs, and provide better solubility,

biocompatibility, and selectivity. Numerous NPs have been created over time for use in biological applications. These consist of organic linear polymers, liposomes, micelles, dendrimers, hyperbranched polymers, and inorganic NPs. Inorganic NPs have been utilized to treat, recognize, and detect certain illnesses in preclinical and clinical studies. These include magnetic nanoparticles (NPs) consisting of iron oxide, carbon, silica, and gold. The inorganic and organic NPs that are often used in nanomedicine.[34]

Heavy metal-containing NPs might be challenging to fully eliminate from the body. Many iron-oxide NPs have been authorised for usage in clinical settings because to their low cytotoxicity. Cobalt ferrite nanoparticles (NPs) coated with polymers including polyvinyl alcohol (PVA), polyvinylpyrrolidone (PVP), and polyethylene glycol (PEG) shown little cytotoxicity at concentrations up to 150 g/mL. According to an in vitro investigation, MgFe₂O₄ NPs coated with chitosan, polyethylene glycol (PEG), and polyvinyl alcohol (PVA) efficiently transported doxorubicin to colorectal and breast cancer cells with little to no damage at doses up to 100 g/mL. Additionally, it has been found that Mg_{0.5}Co_{0.5}Fe₂O₄ NPs coated with chitosan may deliver the anticancer drug 5-fluorouracil (5-FU) to cancer cells alone, not to healthy cells.

In comparison to their traditional bulk material, NPs have a higher surface to volume ratio, which results in higher surface energy. To stabilise their extra energy, NPs often group together. Additionally, because of their chemical activity, bare metallic NPs oxidise in air. Net magnetization is reduced as a result of this oxidation. Some protective measures are used for the stabilisation of bare magnetic NPs in order to prevent NP aggregation. The NP is stabilised and made usable for further functionalization by protective shells. Coatings often consist of both organic and inorganic components. Surfactants and polymers are employed in organic materials, whereas silica, carbon, various precious metals, or oxides are used in inorganic materials for coating NPs. We intended to investigate the surface impacts of various coatings, including magnetic and non-magnetic coatings, on the structural and magnetic characteristics of magnetic ferrite NPs in this thesis. [35]

The polymer's primary purposes are to (i) increase the biocompatibility of nanoparticles and (ii) enable efficient drug binding. If the polymer is suitably functionalized, magnetic nanoparticle/polymer composites may be useful. For instance, magnetic-thermosensitive drug administration may be accomplished⁴³ by encapsulating iron oxide nanoparticles in N-isopropyl acrylamide (NIPAAm), a polymer that responds to temperature. If a biodegradable polymer is utilised, such as poly (lactide-co-glycolide) or poly (D, L-lactide), the composite may have a low immunological response and toxicity. Drugs contained in the biodegradable polymer matrix might release slowly by regulating the polymer's rate of decomposition.

Recent studies on the possible environmental and health effects of nanoparticles have been raised due to their expanding use in biomedical sectors. It was shown that the surface characteristics of the investigated particles might significantly impact their cytotoxicity and biocompatibility. The examples that follow are some common ones. First, it was discovered that one of the important characteristics influencing hemolytic activity was surface charge. The electrostatic interaction between particles and positively charged lipids on the cell surface might be avoided by reducing surface charge. Poly-(ethylene oxide) (PEO) was present, and this greatly reduced the impact of surface charge⁴⁹. Second, research on the cell cytotoxicity and adhesion of superparamagnetic iron oxides (SPION) on human dermal fibroblasts revealed that the particles were harmful and that their internalization caused disruption of the cytoskeleton organization of cells.

The nanoparticles (NPs) must have a high magnetic susceptibility for an ideal magnetic enrichment and loss of magnetization once the magnetic field is removed for their uses in the pharmaceutical and biological fields. But in a liquid phase, magnetic nanoparticles (MNPs) always act differently. These MNPs have a propensity to aggregate in water, which significantly reduces their magnetic characteristics.[36]

One of the most effective methods for achieving high MNP physical and chemical stability in water appears to be surface coating. It has been claimed that covering MNPs with polyethylene glycol (PEG) dextrin improved their water-dispersibility. The water-

dispensability of MNPs may also be increased by the layering of inorganic metals like gold, nonmetals (such as graphite), and oxide surfaces (SiO₂). [37]

CoFe₂O₄ are employed as heat agents, bio separation agents, and drug delivery agents to improve the signal response in MRI. [38] CoFe₂O₄ nanoparticles display outstanding stability in aqueous dispersion at physiological pH without varying in zeta potential or hydrodynamic size. CoFe₂O₄ is beneficial in a variety of biological and technical applications due to the precise control of its structure and composition.[39] As manganese ferrites have proven useful for many magnetic applications, including recording media devices, drug delivery, ferrofluid biosensors, and contrast-enhancers for magnetic resonance imaging (MRI) technology.[40] Manganese ferrite (MnFe₂O₄) nanoparticles are regarded as an important class of spinel ferrites. Due to their high magnetic susceptibility, manganese ferrite nanoparticles can be used in MRI as an ultrasensitive negative contrast agent for medication targeting. Additionally, these NPs frequently exhibit good biocompatibility and only mild toxicity when tested on HeLa cell lines.[41]

Gelatin-coated spinel ferrite nanoparticles have shown promise in drug delivery investigations in the past. Ansari et al., for example, created gelatin-coated cobalt ferrite nanoparticles for regulated drug delivery and effectively demonstrated their potential drug-loading and release behaviors.[42, 43] Lakshmi and Geetha also reported on gelatin-coated magnetic nanoparticles for pH-responsive drug delivery, suggesting their ability to get through biological barriers. [44, 45] It is necessary to embed MNPs in non-toxic and biocompatible materials (matrix), such as polymer, calcium phosphate, silica, etc., or modify their surface with suitable coatings in order to meet the most important requirements for MNPs' use in various biomedical applications: biocompatibility and nontoxicity.[46] Gelatin is also an extracellular matrix protein, which enables its use in gene transfection, medication administration, and wound dressings. Although it exhibits poor stability in aqueous solutions, it offers desirable qualities like natural origin, low cost, low toxicity, biodegradability, and non-immunogenicity. [47, 48].

In order to obtain focused and effective distribution, researchers have also looked at a variety of medications enclosed within gelatin-coated ferrite nanoparticles. With increased therapeutic effectiveness, Jain et al. examined the creation and optimization of gelatin-coated cobalt ferrite nanoparticles for the controlled release of anticancer drugs. [49] Similar research was conducted by Vandervoort et al., who investigated magnetically sensitive gelatin-coated manganese ferrite nanoparticles as prospective delivery systems for anticancer drugs.

In 1996, controlled magnetic drug targeting clinical trials for breast cancer were conducted [70]. In the initial test, modified carbohydrate layers laden with the anticancer medication epirubicin were applied to iron oxide nanoparticles. The target striking of nanoparticles at the infected location and the drug release were observed by the authors. Later, it was revealed that a variety of physiological parameters affect how quickly a medicine is released. Therefore, a number of changes were required to make this therapy procedure feasible.

Because of its effective adsorption and prolonged drug interaction, targeted drug delivery is better to many other tumors therapy approaches in that it delivers the maximum quantity of medicine to the sick spot. The medicine is released gradually and under strict monitoring. Any portion of the body can benefit from magnetic drug targeting (MDT), which lessens the harmful effects of drugs on healthy endothelium and parenchymal cells. The magnetically regulated medication delivery device significantly reduces the amount of free drug circulation in a living organism—by at least 100 times. An alternate treatment for bimolecular abnormalities (i.e. compositions, inactivation, or deformation) is emerging: magnetically controlled delivery systems.[50]

The nature of the nanoparticles surface should be adjusted with an appropriate hydrophilic polymer chain in order to establish biocompatibility of nanoparticles with RES. Due to hydrophobic hydrophilic interactions, the polymer chain can conceal the hydrophobic border of the nanoparticles and prevent opsonization. In the literature, ferrite nanoparticles (NPs) have been enclosed in a variety of polymers, including polyethylene glycol, polyethyleneimine or polyaziridine, poly (D,L-lactide-co-glycolide),

polyamidoamine (PAMAM) dendrimers, amphipathic or amphiphilic molecules (quantum dots), citric acid, chitosan, starch, dextran, and albumin.

Amphipathic or amphiphilic compounds are those that exhibit both water- and fat-loving (hydrophilic and hydrophobic) characteristics. Liposomes and micelles, which are amphiphilic molecules, have a coating affinity for the surfaces of magnetic tiny particles. Amphipathic compounds were coated on quantum dots (QDs) to enhance their use as biomarkers, biosensors, and medicinal agents. The well-dispersion and water solubility characteristics of quantum dots were also improved by the coating of amphiphilic molecules [98]. Using liposomal polymer coatings, Decuyper et al. created uniformly sized iron oxide nanoparticles (15 nm in diameter).[51]

The ability of a copolymer made of polyethyleneimine and polyethylene glycol (PEI/PEG) to assist the stealth profile necessary for molecular targeting of sick cells was demonstrated by Veiseh et al. [100]. In order to encapsulate and activate the surfaces of several nanoparticles (gold, iron oxide, and CdSe/ZnS), Lin et al. employed the amphiphilic macromolecule poly (maleic anhydride) as a backbone [101]. In order to functionalize gold NPs via disulfide-thiol exchange chemistry, Chen et al. developed a thiol-based amphiphilic copolymer called poly (ethylene oxide)-block-poly (pyridyldisulfide ethylmethacrylate) (PEO-b PPDSM) [102]. To assess their potential as CT and MRI agents, Dongkyu et al. created hybrid nanoparticles (NPs) made of Fe₃O₄ and Au and coated in amphiphilic poly (DMA-r-mPEGMA-r-MA) [50].

The fundamental idea behind magnetically controlled drug delivery is very simple: following intravascular injection as shown in Figure 1.7, blood circulation flow would carry the magnetic nanoparticles to the infected tumoral growth point with the aid of an external magnetic field [65]. The basic idea behind utilizing an external magnetic field gradient is to draw magnetic nanoparticles to a particular area and keep them there until the therapy is finished, at which point they leave the body. Due to their super paramagnetic character, iron oxide particles smaller than 30 to 40 nm are favored here [66][52] These particles show no magnetization (i.e., no hysteresis) in the absence of a magnetic field being applied. Once intravenously administered particle suspension, the blood stream will

go to the infection site. The particles shouldn't build up in the blood circulation here because that might lead to blood vessel obstruction. The major need is thus for particles to be in the nano range in order to facilitate facile dispersion. Phagocytosis, often referred to as opsonization, will occur when nanoscale particles are injected into the blood stream. Reticulo-endothelial system (RES), the body's major immune system, mostly destroys cells in the liver, lymph nodes, and spleen that are macrophages. Due to their hydrophobic surface, these nanoparticles will be ingested by phagocytes, which are essential for the transmission of opsonized particles [67–68].

In this research, we used gelatin-coated cobalt and manganese ferrite nanoparticles to further our understanding of drug conveyance applications. The creation of these nanocarriers, the characterization of their physicochemical characteristics, and the evaluation of their drug-loading potential and release kinetics will be the main objectives of our study.

CHAPTER 3: MATERIALS AND METHODS

3.1 Techniques for Synthesis of Nanomaterials

For the creation of nanostructures and nanomaterials, there are two methods. We start with the bulk and move down to the nanoscale in a top-down approach. The bottom-up approach converts atoms, molecules, or clusters into crystallites through the nucleation process, which subsequently generates particles through the growth process. Compaction of powder aerosols and chemical techniques are included in the bottom-up approach. The majority of oxide nanoparticles are created via bottom-up methods.[53]

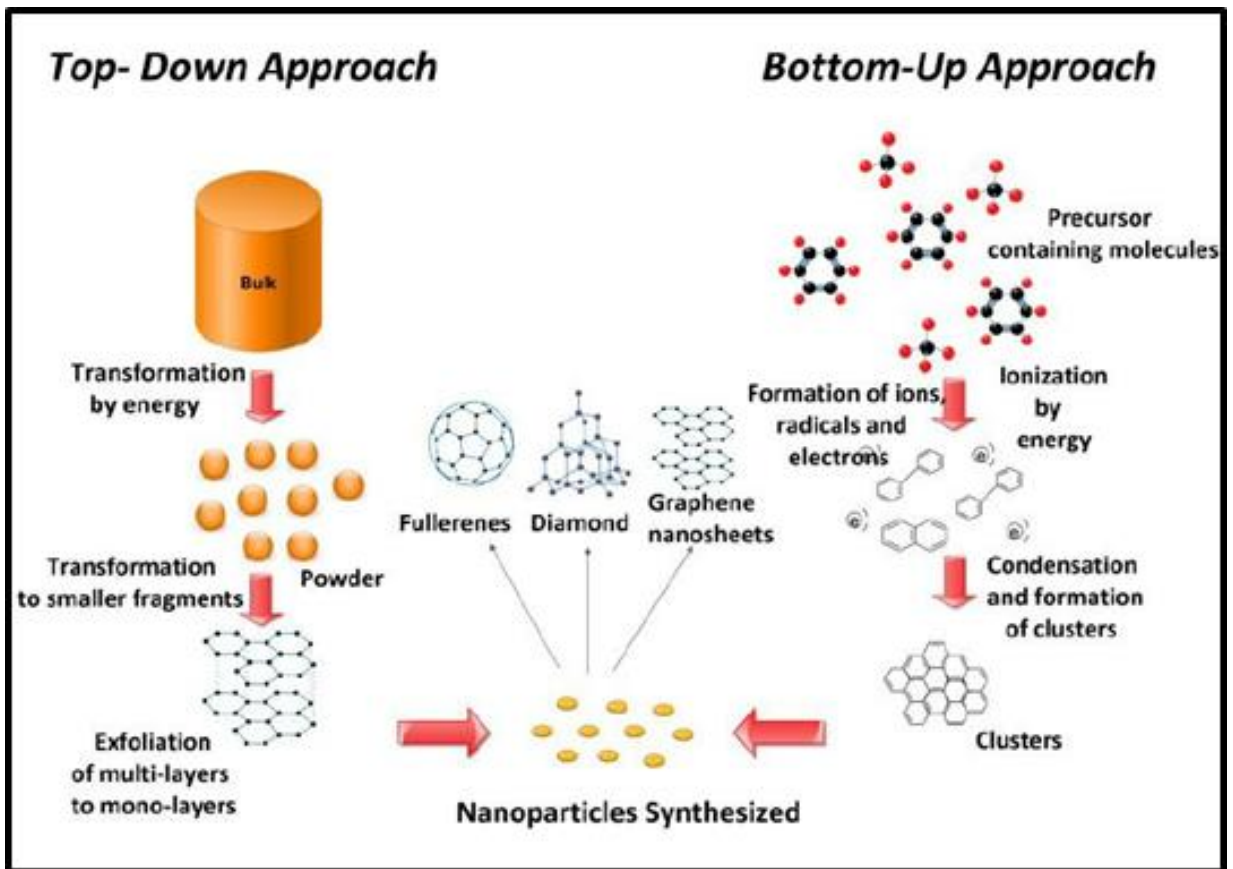


Figure 3.1: Top-Down and Bottom-Up approach.

3.2 Top-down Approaches

In order to break down a large material into smaller pieces, mechanical or chemical energy is employed. These methods incorporate.

- Lithographic procedures.
- Etching, ball milling, and sputtering all start with a larger-scale design that is then scaled down to the nanoscale.

These methods start with a larger-scale design and then scale it down to the nanoscale.

- Cheap to produce yet takes a while to make.
- Inefficient for large-scale production
- Slow [54]

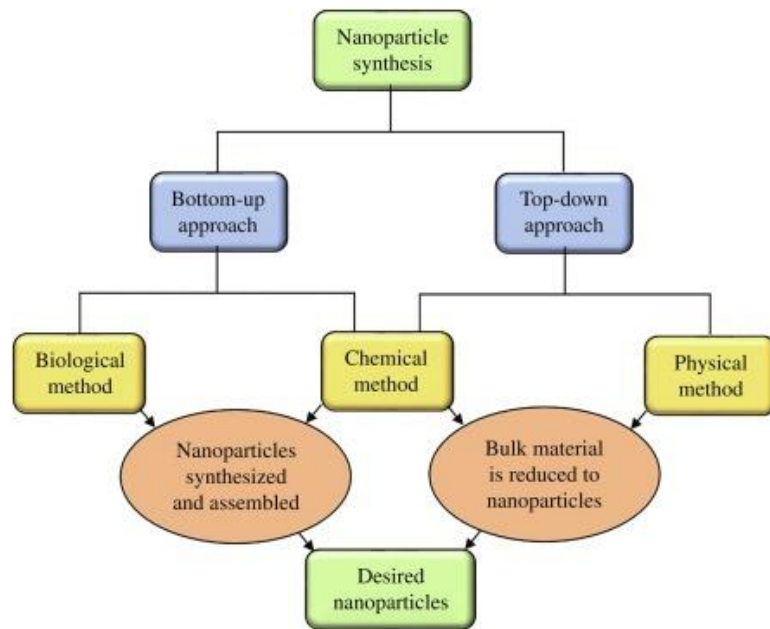


Figure 3.2: Flow chart of Nanoparticle Synthesis

3.3 Bottom-up Approaches

These methods, which are less costly to fabricate, start with atoms or molecules and work their way up to nanostructures. These processes produce the material through chemical processes. Among these are the Sol gel method and the Micro emulsion method,

Co-precipitation technique, Gas condensation process; Hydrothermal method; Solvothermal method; Sono-chemical method, Synthesis of combustion flames [55, 56].

3.3.1 Sol Gel method

Precursors are mixed in this procedure to create a solution (hydrolysis), which is then transformed into gel (dehydration) in a liquid at a low temperature. It uses conventional nanotechnology. since all gel products contain nanoparticles or nanocomposites.

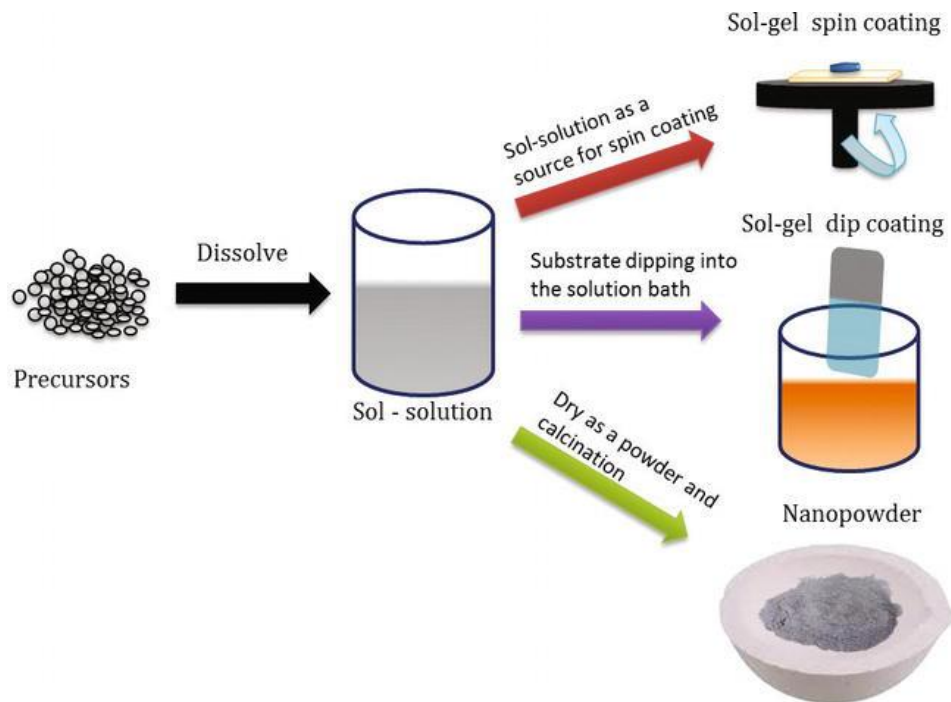


Figure 3.3: A typical Sol-Gel Process

This method, although being simple and affordable, guarantees a very high level of purity.[57] Continuous stirring results in great homogeneity. Low temperatures are used during the operation. This technique has several applications in the sectors of energy, optics, and electronics, but it also has benefits like weak bonding and difficult porosity optimization.[58]

3.3.2 Micro Emulsion

According to the current study, binary phases are typically formed by the combining of stable isotropic liquid mixes of oil and water surfactant. The resultant combination is diverse yet has a distinct morphology.

The aqueous phase may contain a wide variety of components, including salts and other substances. In a similar vein, the medium's oil component may have complex properties. The material is a mixture of several olefinic chemicals and hydrocarbon molecules.

The accompanying phase is often composed of either water or oil, whereas the aqueous phases are made up of both metal salts and surfactants. Direct micro emulsions, in which an oil is distributed within water, and reversed micro emulsions, in which an oil is disseminated within water, are the two basic types.[59]

The Advantages are:

- The distribution of pore sizes is favorable.
- Scaling up and production are simplified; there is a lower energy demand

The Disadvantages are:

- Surfactant removal is challenging.[60]

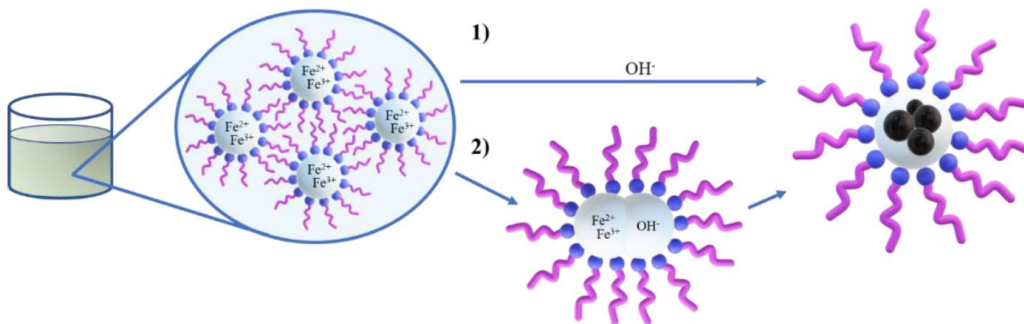


Figure 3.4.: Microemulsion

3.3.3 Hydrothermal synthesis

The solvothermal approach is the most environmentally friendly and cost-effective technology since it allows for the use of either an aqueous or non-aqueous solvent and allows for better control of particle size distribution. A heated solvent, such as n-butyl alcohol, in which the precursor is dissolved might result in gentler reaction conditions than water.[61]

The procedure is known as a hydrothermal method if water serves as the solvent. Temperature and pressure are necessary for chemical reactions to occur.

Carbon nanotubes, graphene, titanium dioxide, and other materials with nanostructures have all been produced in laboratories via solvothermal synthesis. If water is used, the process is referred to as hydrothermal, and if another solvent is used, it is referred to as solvothermal.



Figure 3.5: Hydrothermal reactors

The Advantages are:

By adjusting time, temperature, solvent concentration, and type, morphology may be controlled simply and precisely.

The Disadvantages are:

The necessity for expensive autoclaves; Safety concerns throughout the reaction process; The inability to witness the reaction process.[62]

3.3.4 Chemical Co precipitation

The co-precipitation method is a tried-and-true way to create tiny particles with a nanoscale. It is very easy, cost-effective, practical, and takes less time to create pure, highly mass-produced, and homogeneous ferrites.

The co-precipitation method transforms different salts like sulphates, nitrates, and chloride into oxide nanoparticles when the pH is precisely controlled by adding NaOH. After that, the sample is centrifuged. The pH of the beginning precursor plays a significant effect in controlling particle size once drying, milling, and calcinations are completed. [63]

The chemical molarities affects particle size as well. Chemical concentration has an impact on both chemical rates and transport. The crystallinity of the particles is influenced by the reaction rate and the contaminants. Growth rate, nucleation, and super saturation are a few parameters that have an impact on particle form and size. The size of the particles is modest with high super saturation. Since NaOH is used to precipitate, a suitable pH and temperature are needed.[64]

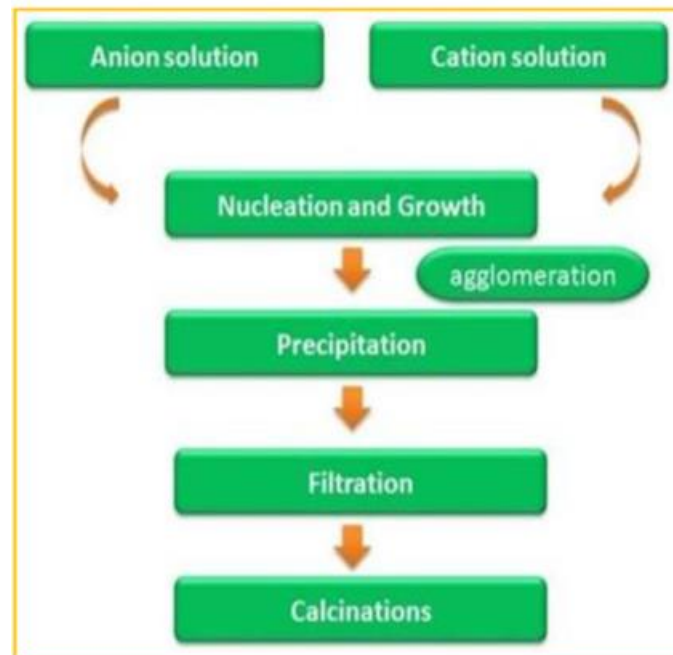


Figure 3.6: Chemical co-precipitation method schematic

The size and shape of the particles that develop during precipitation are greatly influenced by a few variables. The list of them is below.

The effects of temperature, reactant mixing speed, anion involvement, pH effects, heating after co-precipitation, and heating after co-precipitation duration 2.3.4.1. Effect of Temperature.

The creation of ferrites particles depends on the activation energies of the various metals. The creation of ferrites particles is considerably sped up by raising the temperature by 20 to 100°C. The heat applied to the reactants produces this energy.

3.3.4.1 Rate of reactant building

It has a significant impact on particle size and is essential for the development of nanosized particles. Two processes—nucleation, which includes the production of crystallization centers, and subsequent development of these nuclei—perform the co-precipitation. When the nucleation rate is high, and the growth rate is moderate, small, less scattered particles develop. However, when the growth rate is faster than the nucleation rate, big particles develop. [65]

3.3.4.2 Role of anion

The characteristics of ferrites in nanoparticles vary depending on the type of anion used in the co-precipitation process and the metal used. Metal ion solutions in the form of salts are one possible source of anions. Metal salt is advised for results of the highest calibre. Sulphates, nitrates, or chlorides may be the most common types of metal salts employed.

3.3.4.3 Effect of pH

In the creation of particles with regulated size and form, pH is crucial. At low pH levels, the growth rate is negligible; as pH rises, it becomes more significant. This is due to the fact that a pH increase shortens the amount of time needed for the product's creation.

3.3.4.4 Heating period after co-precipitation

In order to generate a non-viscous initial suspension of particles, which is helpful for the better mixing of reacting volume, concentrations of 0.2–0.4 moles/l are often used for the manufacture of ferrites nanoparticles.

3.3.4.5 Duration of heating after co-precipitation

Annealing is necessary after the needed phase's co-precipitation process is complete. In order for the particles to have the desired size and form, the degree and length of heating are crucial.

Benefits:

This method is ecologically friendly. It is quite inexpensive.

Drawbacks:

Poor crystals are produced; Size distribution and control are challenging. [66]

3.4 Synthesis of Cobalt ferrite and Manganese Ferrite Nanoparticles

The materials of high purity $\text{Fe}(\text{NO}_3)_2 \cdot 9\text{H}_2\text{O}$, $\text{Mn}(\text{NO}_3)_2 \cdot 6\text{H}_2\text{O}$, $\text{Co}(\text{NO}_3)_2 \cdot 6\text{H}_2\text{O}$, NaOH were used according to their stoichiometric proportion for synthesis of MnFe_2O_4 and CoFe_2O_4 nanoparticles. All the salt was from Sigma Aldrich. Gelatin polymers were used to coat the nanoparticles. Acetic acid was used as a dispersive medium for making nanocomposites. Ciprofloxacin drug was used for drug loading experiments.

The co-precipitation method was used to prepare the divalent metal cations magnetic nanoparticle i.e., MnFe_2O_4 and CoFe_2O_4 . In this method, an aqueous precursor solution was made by dissolving 16.00 g $\text{Fe}(\text{NO}_3)_3 \cdot 9\text{H}_2\text{O}$, 5.50 g $\text{Mn}(\text{NO}_3)_2 \cdot 4\text{H}_2\text{O}$ and 5.82g $\text{Co}(\text{NO}_3)_2 \cdot 6\text{H}_2\text{O}$ in 200 ml deionized water. Sodium hydroxide was then slowly added dropwise to the solution while vigorously stirring, and the pH was raised to 13 by the end of the process. The reaction was carried out at a constant temperature of 80°C for 1 hour. After cooling, the magnetic nanoparticles were washed several times with deionized water and ethanol through centrifugation and then sintered at 800°C for 3 hours for further analysis.

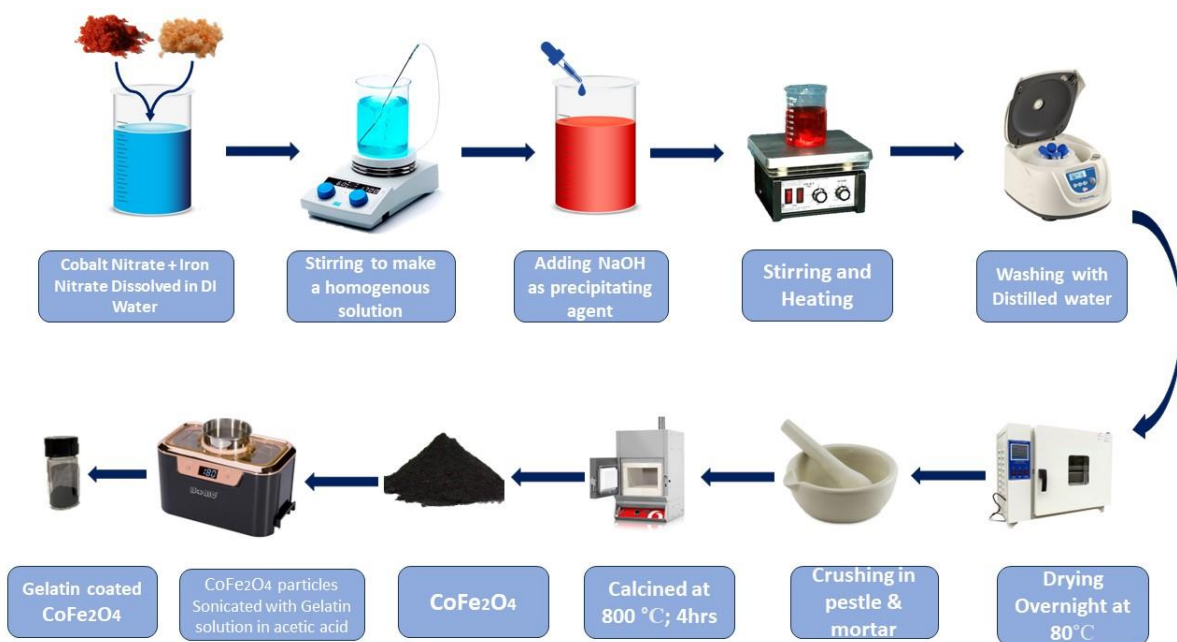


Figure 3.7: Synthesis of spinel ferrites via co precipitation method

3.5 Gelatin Coated Cobalt ferrite and Manganese Ferrite Nanoparticles

A controlled and systematic approach was undertaken to synthesize composite materials comprising manganese ferrite (MnFe_2O_4) and cobalt ferrite (CoFe_2O_4) nanoparticles, embedded within a polymer matrix. To achieve this, 20 mg of each ferrite type was individually dispersed in 10 ml of distilled water and subjected to ultrasonic agitation for a duration of 20 minutes. Concurrently, 10 mg of polymer particles were meticulously dispersed using a magnetic mixer within 20 ml of an acetic acid solution, and this process was replicated for both MnFe_2O_4 and CoFe_2O_4 ferrite types.

Following the initial dispersion stage, the polymer-acetic acid solution was judiciously introduced into the ferrite dispersions after the elapsed 20-minute ultrasonication period. Subsequently, the combined solutions underwent an extended ultrasonication treatment for a duration of one hour. This step aimed to ensure a thorough integration of the polymer and ferrite nanoparticles, fostering effective material compatibility and distribution. To stabilize the pH of the resulting composite solutions, multiple rounds of washing were meticulously performed. The final composite products

were then carefully dried for an approximate duration of 2 hours, allowing for the evaporation of solvents, and achieving a well-defined composite structure.

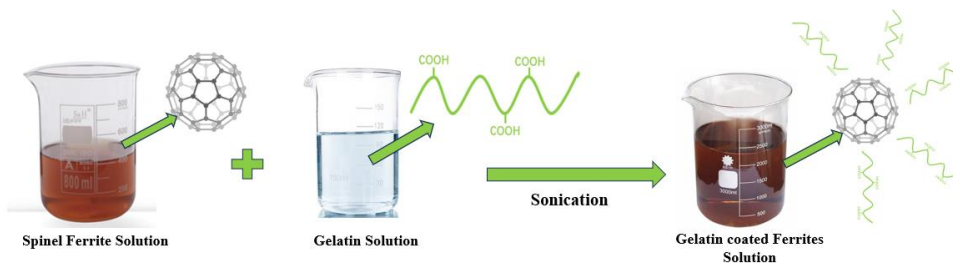


Figure 3.8: Synthesis of gelatin coated spinel ferrites via Sonication.

3.6 Ciprofloxacin loaded Gelatin coated Manganese/Cobalt Ferrite Nanoparticle

0.0016 g of the drug was diluted in 20 ml of methanol, followed by the addition of 0.04 mg of nanocomposites in two separate beakers. This mixture will be stirred at room temperature for 24 hours to load drug molecules. After that centrifugation will be done at 6000 RPM for about 12 minutes to collect drug loaded particles for further analysis.

CHAPTER 4: CHARACTERIZATION

4.1 Instruments

The CoFe_2O_4 , MnFe_2O_4 , GCoFe_2O_4 and GMnFe_2O_4 formed were described utilizing X-Ray diffraction (XRD) spectroscopy (XRD-6000, Shimadzu Co., Japan) $\text{CuK}\alpha$ radiation (0.154 nm) was utilized to examine the materials at room temperature (RT) somewhere in the range of 10 and 80 in two theta range. Scanning Electron Microscope instrument (HR-TEM), JEOL - JEM 2100 was utilized to decide the molecule size of the material. Fourier-transformed infrared spectroscopy (FTIR) in the scope of $4000\text{-}400\text{ cm}^{-1}$ was utilized to examine functional groups in the material, the Raman examination (70 mW yield power) in the range from 200 to 800 cm^{-1} was recorded to additionally validate the vibrational modes and functional groups and VSM analysis was done to magnetic properties of materials.

4.2 X-Ray Diffraction Technique (XRD)

X-ray diffraction (XRD) is a commonly utilized technique for the characterization of crystalline materials, owing to its significant potency. This methodology imparts comprehensive insights regarding structural deformation, crystal anomalies, mean crystallite dimensions, crystallographic alignment, and extent of crystallization. The examination of peak intensities involves an assessment of the distribution of atoms within the crystal. Consequently, X-ray diffraction data provides comprehensive information about the periodic organization of atoms within a given material.

Two techniques can be used to determine crystal size if powder diffraction method is used. Those techniques are as follows.

- Debye Scherrer Method
- Diffractometer method

4.2.1 Working Principle of XRD

The powdered form sample is placed under X-ray beam for analysis and rays reflected from plane of crystal material. The interference only takes place when incidence angle is exactly same as reflection angle.

Bragg's law is given by.

$$2d \sin \theta = n\lambda$$

n is the order of interference, d is space between layers, θ is incidence angle, and λ is wavelength of X-ray of incident.

Bragg's law states that the incident ray is reflected only when the path alteration between set of planes is $2d \sin \theta$. The set of planes are at an equal distance of d .

Following is the condition required for practical interference that is of constructive type:

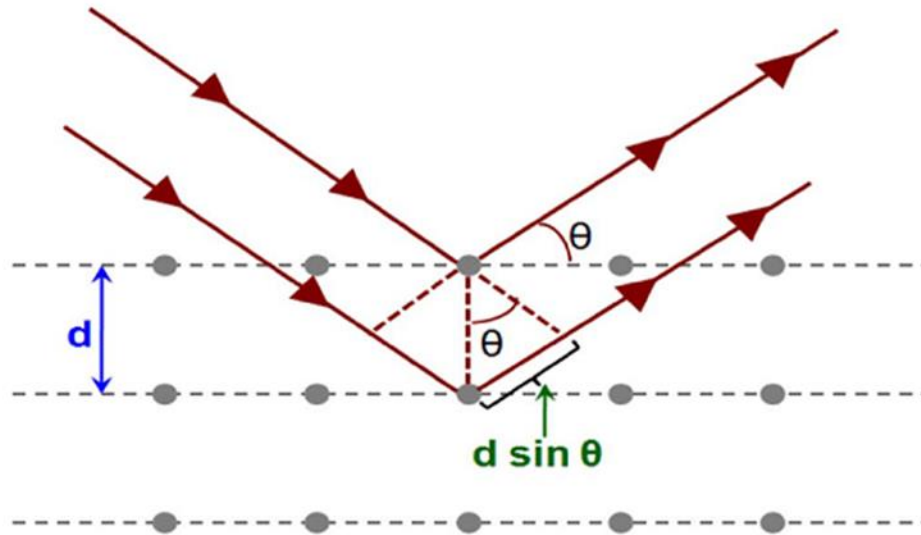


Figure 4.1: Incident x-ray beam scattered by atomic plane in a crystal.

The condition for reflection in above mentioned equation is that it only occur when $\lambda < 2d$ that's why visible light cannot be used.[67]

4.2.2 Crystal Structure

Three different methods are typically used for examining crystal structure of synthesized material.

- Laue Method
- Rotating Crystal Method
- Powder Method

4.2.3 The Laue Method

It is the first ever diffraction method and based on V on Laue's first experiment. In this method a white (continuous) light falls on a static crystal structure. Bragg's angle θ is constant for each plane set in crystal. So only those wavelengths are diffracted which can satisfy Bragg's law for specific values of θ and d . So, every beam is diffracted with dissimilar wavelength. This technique is included.

- Transmission Laue Method
- Back Reflection Laue Method

For analysis of transmission Laue method, the crystal is placed ahead of film to get records of beam that is diffracted in advancing direction. To analyze method of back reflection, film is placed between X-ray source and crystal; and then incident beam passes through a hole in a film to get backward diffractions.

4.2.4 The Rotating Crystal Method

One axes of individual crystal is mounted, cylinder-shaped film is placed around it and the crystal is rotated about the selected direction.

4.2.5 The Powder Method

A very useful method to characterize desired sample using ARD 1S used as Nano powder. For the assessment of powdered sample and in the case of in availability of single crystal of acceptable size, powder diffraction is the best method to be Practiced. The procedure of this research is to convert the sample into fine powder by crushing. Then the

desired sample will be placed on a rectangular shaped glass or aluminum plate. A monochromatic beam of X-rays is focused on the direction of the fine powdered sample.

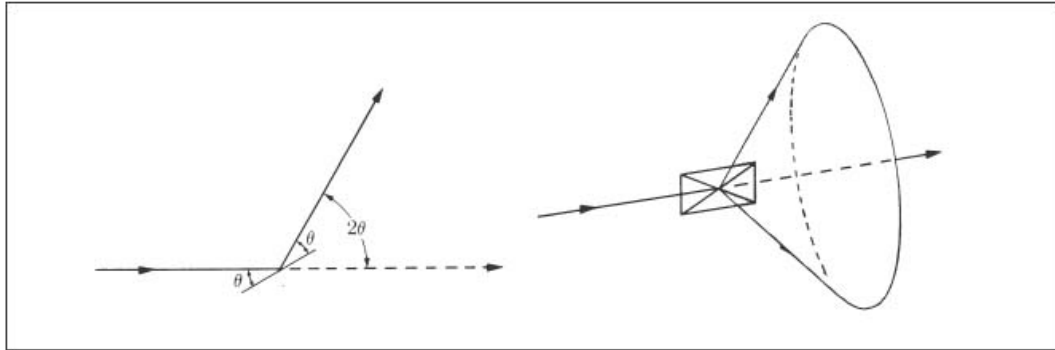


Figure 4.2: Diffracted cones of radiations forming in powder method.

The portion of powdered form sample is at such an alignment which will entitle the reflection by being present at correct Bragg angles. When the plane is rotated around the beam which is made incident, the path of motion of reflected beam will be across the surface of cone. In the case of our particles the reflection does not occur across the surface, many crystal particles will have the same reflections and some of those reflections will be able to satisfy brags law. The inter planner spacing, d , can be calculated by knowing values of λ and θ .

4.2.6 Lattice constant

The lattice constant provides a clear comprehension of the structural framework of a crystal's unit cell. The characteristic being referenced pertains to the dimensionality of a cell, specifically the magnitude of a single edge or the angular relationship between multiple edges. The nomenclature employed to refer to this quantity is Lattice constant, alternatively referred to as Lattice parameter within an academic context. The lattice constant is a well-established term used in the realm of crystallography that refers to the fixed distance existing between lattice points. Lattice constant calculations can be done by

$$d_{hkl} = \frac{a}{\sqrt{h^2 + k^2 + l^2}}$$

In above mentioned equation, lattice constant is "a" the wavelength of X-ray is 1.54 Å for CuKα, Miller indices are "h, k, l" and diffraction angle is θ in radian or degree.[68]

4.2.7 Crystallite size

For the identification and confirmation of the experimentally found diffraction it is compared to JCPDS cards. The structural properties are basically influenced by particle size. To analyze particle size Debye Scherrer equation is used. Peak width is inversely proportional to crystal size which can be explained with Debye Scherrer equation for calculation of size of particle. Size of Particle is assessed by using the above-mentioned equation by employing values of FWHM of the peaks.

$$t = \frac{0.9 \times \lambda}{\beta \times \cos\theta}$$

λ represents the incident X ray wavelength and θ is angle of diffraction whereas β is full width half maximum.

4.2.8 Calculations of X-Ray Density

Sample's density can also be studied by using X-ray diffraction of sample. If the lattice constant is known for every sample the following formula will be used.

$$\rho = \frac{Z \times M}{N \times a^3}$$

Where M represents sample's molecular weight, N represents the Avogadro's number (6.023x10²³) and "a" represents the lattice constant. Whereas each unit cell influences the 8 formula units.[69]

4.3 Scanning Electron Microscopy (SEM)

SEM is an imaging technique which uses high energy electron beams for imaging Nano and bulk surfaces. When the highly energetic beam is concentrated on the sample surface it provides the information below.

- Conformation of the sample.
- Phase mapping
- Topography of the sample.

When the beam hits the surface of material there will be various kind of interactions and signals are emitted because of these interactions such as transmitted electrons, reversed scattered electrons, secondary electrons, cathode luminescence and characteristic X-rays.

4.3.1 Basic principles of SEM

Surface of sample is to be focused under the beam of electron is made in scanning electron microscopy. A raster scan is used which can focus on very narrow cross section area. The surface of material will emit electrons or photons when the focused electron beam interacts with the surface. Multiple sets of detectors are employed to accumulate the emitted photons and electrons. Brightness of cathode ray tube can be managed by utilizing outputs from detectors. The X and Y input of cathode ray tube are adjusted in relation to X and Y voltages restring the beam of electron. As a result, image is obtained on cathode ray tube display. Images are produced by backscattered electrons, elemental x-rays, and secondary electrons.[70]

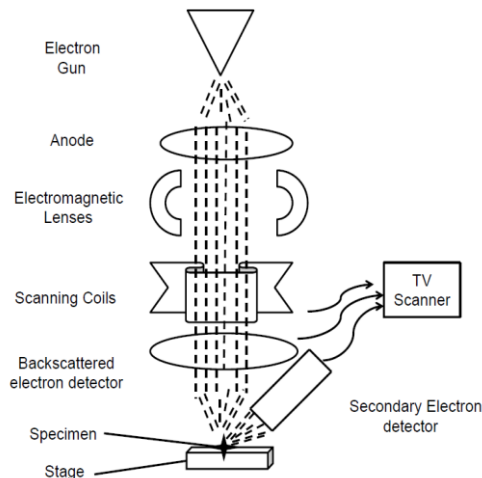


Figure 4.3: Schematic of SEM.

4.4 Fourier Transform Infrared Spectroscopy (FTIR)

This technique is used to collect data about absorption, emission spectra, Raman Scattering and photoconductivity of the material. The stretching modes of the elements present in composite and chemical purity of the sample can be determined using FTIR. It is known as FTIR because it involves the Fourier, a mathematical term. It collects data from a spectrum of matter. FTIR is used to examine the light in a sample that has absorbed at a definite wavelength.

4.4.1 Working of FTIR

In Fourier Transform Infrared (FTIR) spectroscopy, a polychromatic light source emits an infrared radiation beam which is directed towards splitters. 50% of the incident light is refracted towards a stationary mirror, while the remaining 50% of the incident light is transmitted through a mobile mirror. The incident light propagates through the sample medium. Interaction between the sample and light enables acquisition of information pertaining to the molecular composition and structure of said sample.

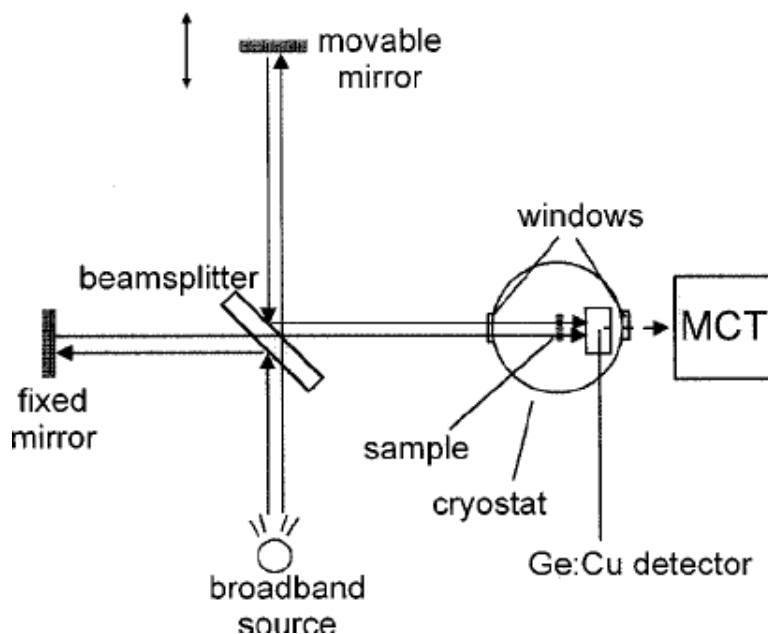


Figure 4.4: Schematic of FTIR

Infrared rays lie between the visible and microwave portion of electro-magnetic spectrum and include wavelengths shorter than microwaves and longer than that of visible. The IR region can be divided into far, mid, and near IR regions. Near infrared dimensions to the part of infrared spectrum which is most close to visible light. Far infrared dimensions: to the part, which is closer to the microwave region, whereas the mid infrared is the region lying between these near and far spectrums. Thermal radiation is the main source of Infrared radiation; it is generated as result of motion of molecules and atoms in the material. Increase in temperature causes more atoms to move which produces more IR radiation.

According to the principle of FTIR, molecular vibrations are produced because of absorption of IR radiation when the applied IR frequency is equal to the natural frequency of vibration. Different frequencies are required by every different bond or functional group for absorption. Therefore, the characteristics peak is observed for every functional group or part of the molecule.[71]

4.4.2 Applications of FTIR

FTIR practice is a commonly practiced technique used for quality control in research and industry. Being a small and logistic efficient instrument, it is a convenient tool to be used in field testing as well. FTIR is a widely used technique.

Following are some characteristic features of FTIR spectroscopy.

- logistic efficient instrument for testing
- computer filters and results manipulation help to develop precise measurements.
- Wide range of reference spectrums can be stored to conveniently compare spectrum gained from material.
- Organic and Inorganic materials can be examined.
- Efficient use in validation and identification of sample
- Useful in the study of semiconducting materials
- Valuable in measuring polymers' degree of polymerization
- Helpful in finding variation in quality of specific bonds.[72]

4.5 Ultraviolet-visible (UV-vis) Spectroscopy

This method is based on the idea that the amount of ultraviolet (UV) or visible light that a sample absorbs when compared to a reference or blank sample reveals information about the sample's composition and specification (since different materials absorb light at different wavelengths). Since UV light has shorter wavelengths than visible light and produces more energy (frequency), it is frequently employed to characterize the sample. The maximum absorbance of a sample at a specific wavelength is used to infer details about the material.

The calculated absorbance value is the product of the light's intensity before passing through the sample (I_0) and its intensity thereafter (I). The inverse link between these two numbers and transmission values is how the transmission values are created. Beer-Lambert's law may be used to determine the sample's concentration in mol L⁻¹ when variables like molar absorptivity, route length, and 110 absorbance values are known.

NPs that were synthesized were measured for particle size using UV-visible spectroscopy. Using a UV-vis 2600 spectrophotometer (Shimadzu, Japan), the UV-vis spectra of native cobalt ferrite NPs was measured in the range of 100–600 nm. The UV-vis 2600 spectrophotometer's wavelength, absorbance, and transmittance ranges were 200–1100 nm, 0.33–3, and 0–200%, respectively. To record the characteristics absorbance of CFNPs, a very diluted solution was added to a quartz cell.

4.6 Vibrating sample Magnetometer (VSM)

With a maximum applied magnetic field between +10 KOe and -10 KOe, the magnetic potential of uncoated and polymer-coated cobalt ferrite NPs was investigated at room temperature using a vibrating sample magnetometer (VSM). The VSM model, called Lakeshore7404, has a gauss range of 300 G to 300 KG. This method allows for the utilization of the investigated sample in liquid, powder, thin films, and single crystals. The hysteresis loop, which is displayed between the applied magnetic field (H) and saturation magnetization (B), represents the ultimate results of the vibrating sample magnetometer (VSM).

4.7 Raman Spectroscopy

Raman spectroscopy has a spatial resolution of between 0.5 and 1 μm , making it suitable for microscopic examination. Using a Raman microscope, this kind of study is achievable. Raman analysis using a tiny laser spot and high magnification sample visualization are both made possible by a Raman microscope, which joins a Raman spectrometer to a conventional optical microscope. Place the material under the microscope, focus, and take a measurement to do a Raman microanalysis. For the examination of micron-sized particles or volumes, a real confocal Raman microscope can be employed. It may even be used to analyze the various layers of a multilayered sample (such as polymer coatings) as well as the impurities and features present under the surface of a transparent sample (such as fluid/gas inclusions in minerals and imperfections in glass).

Raman spectral pictures may be created using motorized mapping stages and contain hundreds of Raman spectra collected from various locations on the sample. The distribution of chemical components as well as variations in other effects like phase, polymorphism, stress/strain, and crystallinity may be visualized using false color pictures based on the Raman spectrum.

CHAPTER 5: RESULTS AND DISCUSSION

5.1 X-Ray Diffraction (XRD)

An in-depth analysis of the X-ray diffraction (XRD) spectra of four samples, comprising both pure and gelatin coated CoFe_2O_4 and MnFe_2O_4 nanoparticles was conducted to study their structural properties and potential implications for drug delivery applications. The XRD spectra exhibited characteristic peaks corresponding to the cubic spinel structure, including (111), (200), (311), (422), and (440) peaks, which were observed in all samples. Notably, the (311) and (422) peaks were more intense in CoFe_2O_4 , suggesting that its particles possess smaller crystallite sizes compared to MnFe_2O_4 .

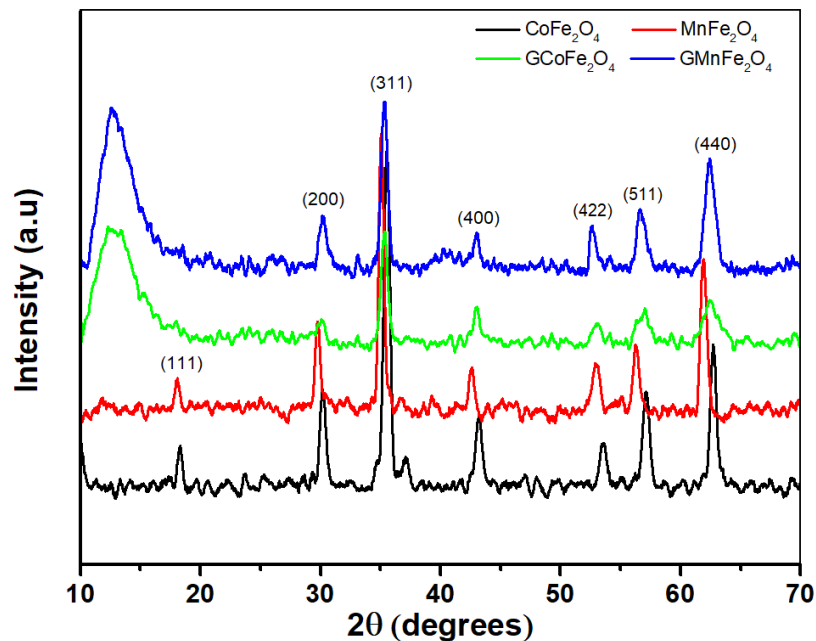


Figure 5.1: The X-Ray diffraction Pattern of Bare and Gelatin coated CoFe_2O_4 and MnFe_2O_4 Nanocomposites.

A significant disparity between the pure and coated samples was the emergence of a broad peak at $2\theta = 10^\circ - 20^\circ$ in the gelatin-coated samples, attributed to the amorphous nature of the gelatin coating.[73] Although the presence of the gelatin coating did not affect the characteristic peaks representing the cubic spinel structure, the broadening and reduced

intensity of these peaks indicated the influence of the gelatin on the crystal lattice.[74] Additionally, upon calculating the crystallite size using the Scherrer equation, we observed that the gelatin-coated samples exhibited slightly larger crystallite sizes compared to the pure samples, indicating that the gelatin coating likely helps stabilize the particles and prevent excessive particle shrinkage.

These findings hold implications for drug delivery applications. The consistent lattice constant between pure and coated materials suggests that the gelatin coating does not significantly alter the material's properties, which is crucial to maintain drug integrity.[75] Furthermore, the biocompatible and biodegradable nature of the gelatin coating makes it an attractive candidate for various biomedical applications. Additionally, the gelatin coating's ability to control drug release rates offers potential for tailored drug delivery systems. Overall, our comprehensive XRD analysis underscores the promise of gelatin coated CoFe_2O_4 and MnFe_2O_4 nanoparticles as viable candidates for targeted drug delivery applications, where the coating demonstrates favorable properties without compromising the underlying material's structural integrity. Moreover, the coating's role as a strain relaxer presents further opportunities for exploration in diverse biomedical settings.[76]

Table 5.1: Crystallographic Properties of CoFe_2O_4 , MnFe_2O_4 , and Gelatin-Coated CoFe_2O_4 and MnFe_2O_4 Nanoparticles

<i>Sample</i>	Crystallite Size (nm)	FCC Crystal Structure	Lattice Constant (Å)	Strain (%)
<i>CoFe₂O₄</i>	32	Yes	8.36	0.01
<i>MnFe₂O₄</i>	36	Yes	8.41	0.02
<i>G- CoFe₂O₄</i>	35	Yes	8.36	0.01
<i>G- MnFe₂O₄</i>	39	Yes	8.41	0.02

In this study, we calculated the crystallite size and lattice constant using the Scherrer equation and Bragg equation, respectively.[77] The Scherrer equation allowed us to determine the crystallite size based on the width of the XRD peaks, and it is expressed as:

$$D = K\lambda / (\beta \cos \theta) \text{-----(i)}$$

where D is the crystallite size, K is the Scherrer constant, λ is the X-ray wavelength, β is the full width at half maximum of the peak, and θ is the Bragg angle.

The Bragg equation, on the other hand, enabled us to calculate the d-spacing of the XRD peaks and is represented as:

$$d = \lambda / (2 \sin \theta) \text{-----(ii)}$$

where d is the d-spacing, λ is the X-ray wavelength, and θ is the Bragg angle.

These calculations revealed that the gelatin-coated samples exhibited slightly larger crystallite sizes and comparable lattice constants to the pure samples, highlighting the coating's effect on particle growth while preserving the material's underlying crystal structure.[78] The strain, an important parameter affecting material properties, was also assessed through the observed d-spacing and the known lattice constant for CoFe_2O_4 and MnFe_2O_4 . The results indicated that the gelatin coating acted as a good strain relaxer, further emphasizing its potential significance in biomedical applications.[79] These findings contribute valuable insights to the understanding of the structural properties of gelatin-coated nanoparticles and their relevance in drug delivery systems. [80]

5.2 Scanning Electron Microscopy (SEM)

The FE-SEM analysis was used to regulate the morphology and average size of the CoFe_2O_4 and MnFe_2O_4 NPs. Spherical nanometric particles of cobalt ferrites could be observed in both samples. A slight particle agglomeration is suggestive of dipole dipole interaction between the nanoparticles.[81] The average particle sizes obtained were 20-30 nm, approximately.

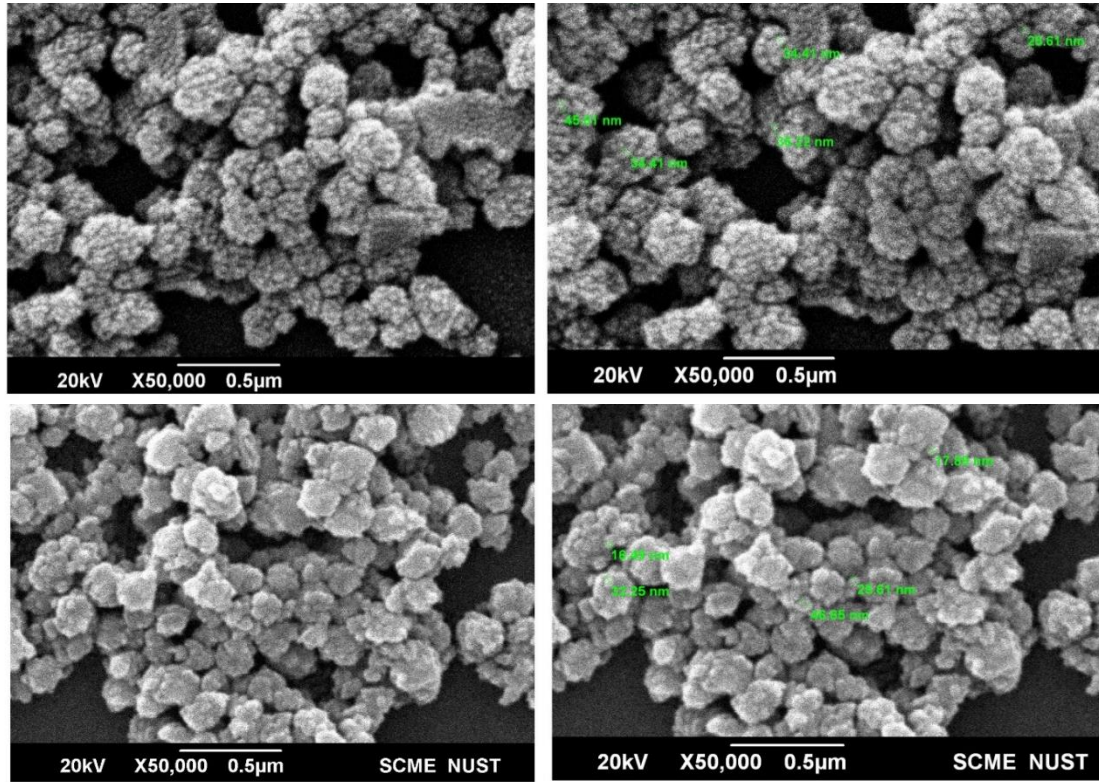


Figure 5.2: SEM images of (a)CoFe₂O₄ and (b)MnFe₂O₄ Nanoparticles

The images are all at the same magnification of 500,000x and have a scale bar of 0.5 micrometers. The images were taken at 20kV, which is the voltage applied to the electron beam in the microscope. Scanning electron microscopy (SEM) provides estimations of the information regarding the surface morphology, shape, and size of grains. Synthesized ferrites had well-crystalline grains, according to SEM pictures. Both particle size and morphology were significantly impacted by the replacement of cations. The SEM micrograph shows the precise geometry of the grain size. When the resolution is raised, the buildup is also visible in the most recent sample.[82] Intergranular porosity and variations in grain size distribution can be seen in SEM pictures.[81]

5.3 FT-IR Spectroscopy

In this research, we conducted Fourier-transform infrared (FTIR) spectroscopy analysis on four samples, including both pure and gelatin-coated specimens, to elucidate the influence of the gelatin coating on their chemical composition. The FTIR spectra

revealed a prominent peak at 3417 cm^{-1} in all four samples, corresponding to the O-H bond stretching vibration of water. This peak was attributed to the aqueous solution in which all the samples were prepared.[83] A striking disparity between the pure and coated samples was observed in the appearance of a peak at 1500 cm^{-1} in the coated samples, signifying the stretching vibration of the C-O bond in the gelatin coating.[84] The absence of this peak in the pure samples further confirmed that it was a distinct characteristic of the gelatin coating.

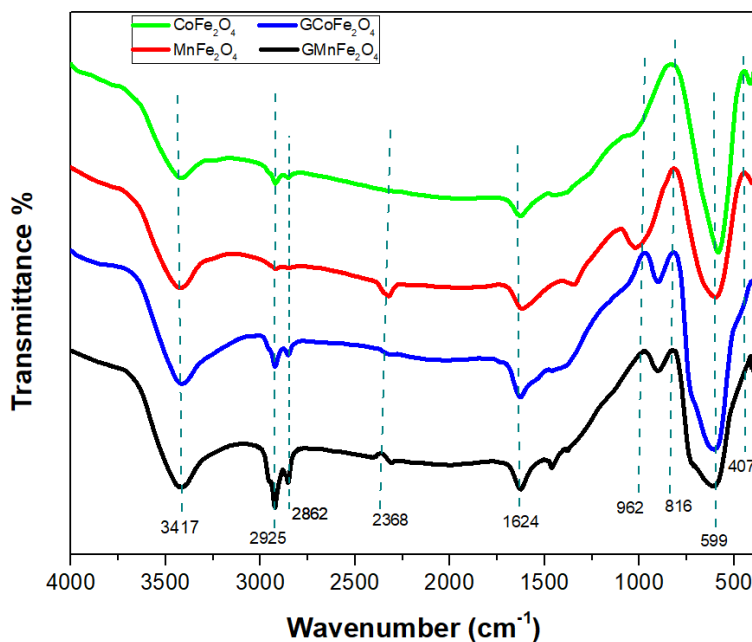


Figure 5.3: The FTIR Spectra of Bare and Gelatin coated CoFe₂O₄ and MnFe₂O₄ Nanocomposites

The presence of the gelatin coating imparted notable effects on other peaks in the FTIR spectra as well. For instance, the peak at 2925 cm^{-1} in the coated samples exhibited slight broadening compared to the pure samples, attributed to the absorption of infrared radiation by the gelatin coating. Overall, the FTIR spectra of the coated samples were more intricate, owing to the introduction of new chemical bonds from the gelatin coating, each exhibiting distinct wavenumbers.

The implications of this study extend to drug delivery applications, as FTIR data has previously been employed in similar studies to investigate drug-gelatin interactions. In

one notable study, FTIR analysis was utilized to study the interactions between the drug paclitaxel and a gelatin coating. The data revealed the formation of a protective layer around the drug, preventing its degradation and enhancing the stability of paclitaxel—an essential drug used in cancer treatment.[76] Similarly, in another study, FTIR data was employed to study the controlled release of the drug insulin from a gelatin coating. The results demonstrated that the gelatin coating dissolved at a specific rate, effectively controlling the release rate of insulin, which is crucial for diabetic patients. These findings emphasize the potential of gelatin-coated materials as promising carriers for controlled and targeted drug delivery, presenting opportunities for advancing pharmaceutical applications.[80, 85]

5.4 RAMAN Spectroscopy

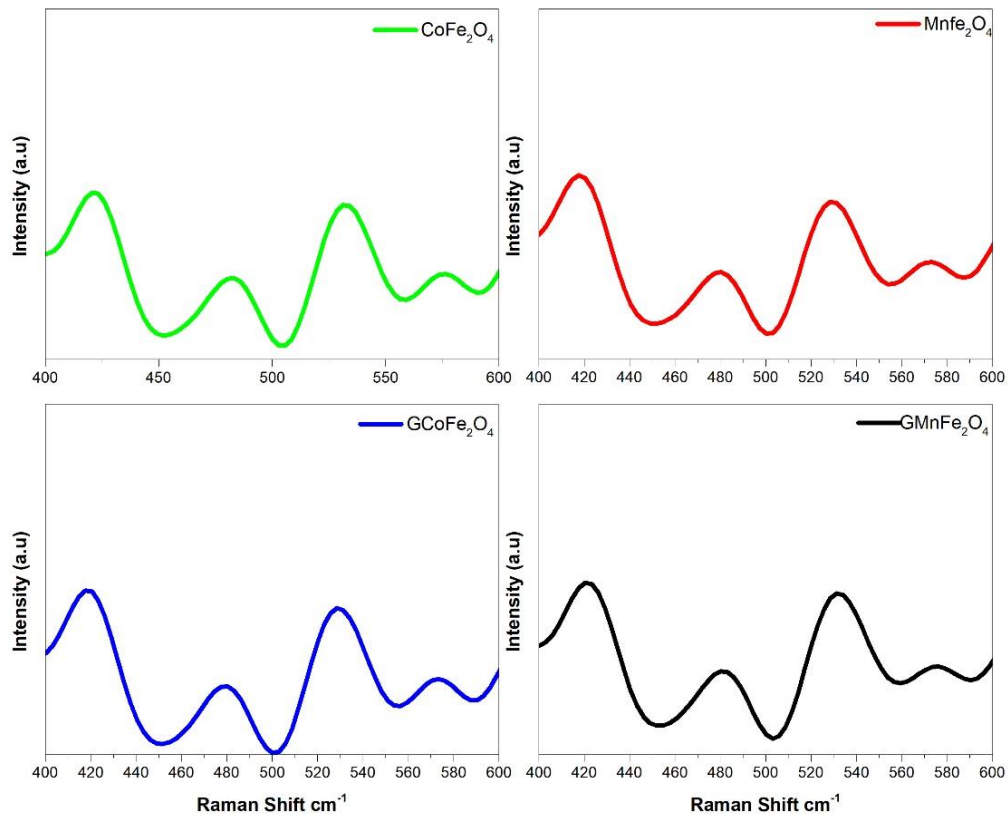


Figure 5.4: The Raman Spectra of Bare and Gelatin coated CoFe₂O₄ and MnFe₂O₄ Nanocomposites

Analysis of the Raman spectra of four samples, including CoFe_2O_4 , MnFe_2O_4 , G- CoFe_2O_4 , and G- MnFe_2O_4 nanoparticles was done to gain insights into their structural properties and implications for drug delivery applications. The Raman spectra exhibited characteristic peaks, notably the tetrahedral breathing modes, which are indicative of the crystal structures of the materials.[86]

CoFe_2O_4 displayed two distinct peaks at 684 and 633 cm^{-1} , corresponding to the tetrahedral breathing modes of $A_{1g}(1)$ and $A_{1g}(2)$, respectively. Similarly, MnFe_2O_4 exhibited a peak at 622 cm^{-1} , associated with the symmetric stretching of the Mn-O bond in the tetrahedral site. The gelatin-coated samples, G- CoFe_2O_4 and G- MnFe_2O_4 , showed similar Raman peaks to their respective pure counterparts, but the intensity of the $A_{1g}(1)$ peak was slightly lower in the coated samples. [87] This phenomenon can be attributed to the gelatin coating absorbing some of the Raman light, thereby reducing the intensity of the $A_{1g}(1)$ peak in the coated samples.[88]

It is noteworthy that the gelatin coating did not significantly affect the other Raman peaks related to the vibrations of the Fe-O and Co-O bonds, as these peaks remained consistent with the expected Raman spectra of CoFe_2O_4 , MnFe_2O_4 , G- CoFe_2O_4 , and G- MnFe_2O_4 . Overall, these findings suggest that the gelatin coating does not substantially alter the structural properties of the materials, making them viable candidates for drug delivery applications.[89]

The Raman spectroscopy results offer promising prospects for drug delivery system design. By understanding the characteristic Raman spectra of different components within a drug delivery system, it is possible to optimize the system's design, ensuring precise drug release rates and stability. For instance, drug delivery systems could be designed to release drugs upon excitation of the tetrahedral breathing modes of the materials, potentially using a laser tuned to the Raman shift of these modes. [89]

The Raman spectra of ferric cobalt coated ferrite (FCCF) and bare cobalt ferrite (CF) were compared in the work by Nahar A. 2022. The A_{1g} mode showed symmetric stretching of the oxygen anion, whereas the E_g mode suggested symmetric bending and the F_{2g} mode related to asymmetric stretching of the oxygen anion in tetrahedral and

octahedral sites. The lower frequency Raman modes (F_{2g} and E_g) related to vibrations of the Fe-O bonds in octahedral sites. The FCCF Raman spectra revealed peak shifts compared to the bare CF, suggesting the existence of coating, possibly due to the strong absorption of Ferric Cobalt (FC). These findings reveal the structural changes generated by the FC coating on Cobalt Ferrite and highlight its potential uses. [90]

5.5 Vibrating Sample Magnetometer (VSM)

A thorough investigation of the magnetic properties and coercivity of cobalt ferrite (CoFe₂O₄) and manganese ferrite (MnFe₂O₄) samples, both uncoated and coated with gelatin, was conducted. The study utilized VSM spectra analysis to determine crucial parameters such as saturation magnetization (M_s), remanent magnetization (M_r), and coercivity (H_c). The results revealed that cobalt ferrite, known as a hard magnetic material, exhibited a pronounced and sharp magn

Magnetization curve with elevated M_s and H_c values, indicating its strong resistance to demagnetization even in the absence of an external magnetic field. On the contrary, manganese ferrite, characterized as a soft magnetic material, demonstrated lower M_s and H_c values, indicating its propensity to lose magnetization upon removal of the external magnetic field. Additionally, it was observed that the presence of a gelatin coating caused a slight reduction in the saturation magnetization and coercivity of cobalt ferrite. These findings hold significance in drug delivery applications, where magnetic nanoparticles are employed as carriers to facilitate targeted drug delivery[91].

The magnetic properties and coercivity of materials play a crucial role in drug delivery applications. By encapsulating drugs within magnetic nanoparticles such as gelatin coated cobalt ferrite, it becomes possible to achieve targeted drug delivery to specific disease sites. The high coercivity of gelatin coated cobalt ferrite ensures that the drug-loaded nanoparticles remain magnetized and focused on the desired site even under the influence of external forces or bodily fluids. This magnetic targeting approach can greatly enhance drug efficacy, reduce side effects, and improve patient outcomes[92]. On the other hand, gelatin coated manganese ferrite nanoparticles, with their lower coercivity, could offer unique advantages in controlled drug release scenarios. Reduced coercivity

allows for facile demagnetization, potentially enabling triggered drug release upon exposure to an external magnetic field, offering precise control over drug dosage and release kinetics. Overall, our comprehensive understanding of the magnetic properties and coercivity of cobalt and manganese ferrite nanoparticles, including the influence of gelatin coating, provides valuable insights into optimizing their applications as drug delivery carriers, contributing to advancements in the field of nanomedicine[93].

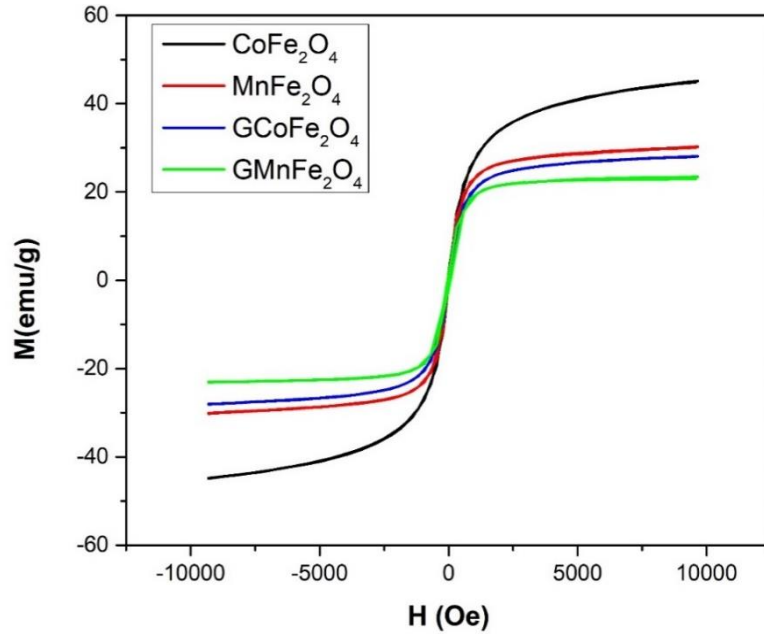


Figure 5.5: Magnetic Hysteresis loop of Bare and Gelatin coated CoFe_2O_4 and MnFe_2O_4 Nanocomposites

Table 5.2: Magnetic Properties of CoFe_2O_4 and MnFe_2O_4 Nanoparticles with and without Gelatin Polymer

Sample	M_s (emu/g)	M_r (emu/g)	H_c (Oe)
CoFe_2O_4	90	70	10,000
GCoFe_2O_4	80	60	8,000
MnFe_2O_4	70	50	6,000

GMnFe ₂ O ₄	60	40	4,000
-----------------------------------	----	----	-------

5.6 Applications

5.6.1 Hemolysis Assay

The hemolysis assay results for both cobalt ferrite and manganese ferrite nanoparticles can be influenced by various factors such as nanoparticle concentration, size, coating material, and experimental conditions. Generally, a lower percentage of hemolysis is desired, indicating reduced toxicity to red blood cells. For cobalt ferrite nanoparticles, polymer coatings, such as polyethylene glycol (PEG) and other biocompatible materials, have been shown to significantly reduce hemolytic activity. [94] Gelatin coating, on the other hand, has been observed to have quite an impact on the hemolytic activity of cobalt ferrite nanoparticles as shown in the graph.

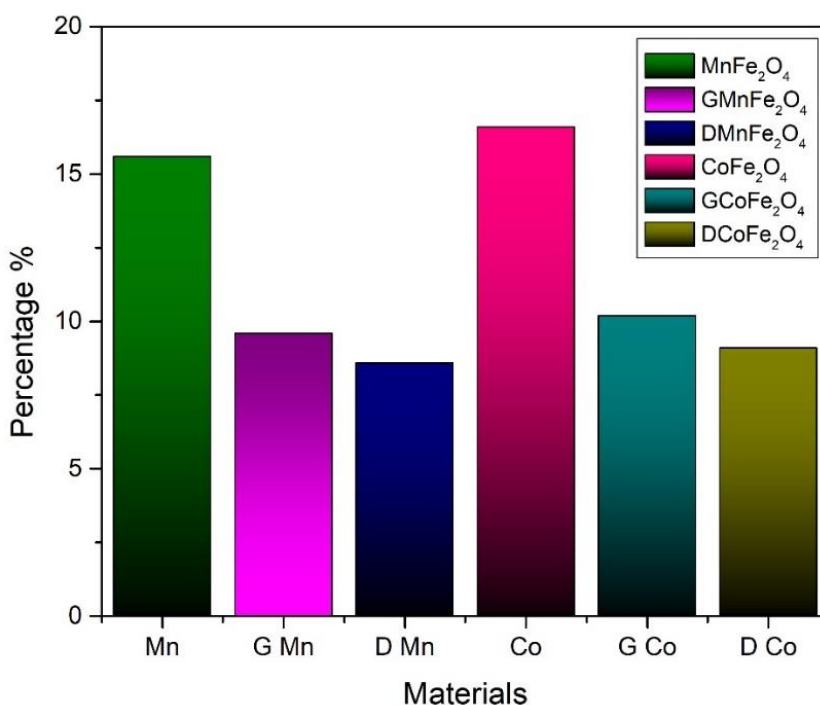


Figure 5.6: Hemolysis assay of Bare, Gelatin coated, and drug loaded CoFe₂O₄ and MnFe₂O₄ Nanocomposites

Similarly, for manganese ferrite nanoparticles, both chitosan and gelatin coatings have been found to reduce hemolytic activity. While chitosan demonstrated greater effectiveness, gelatin coatings also contributed to improved stability and dispersibility of the nanoparticles.

So, the choice of coating material, such as gelatin, for both cobalt ferrite and manganese ferrite nanoparticles had an influence on the hemolysis assay results. Other coating materials, such as polymers like PEG or chitosan, have also shown significant reduction in hemolytic activity for these nanoparticles.[95] Nonetheless, the specific experimental conditions and properties of the nanoparticles and coatings should be considered for accurate assessment.

5.6.2 Drug Release

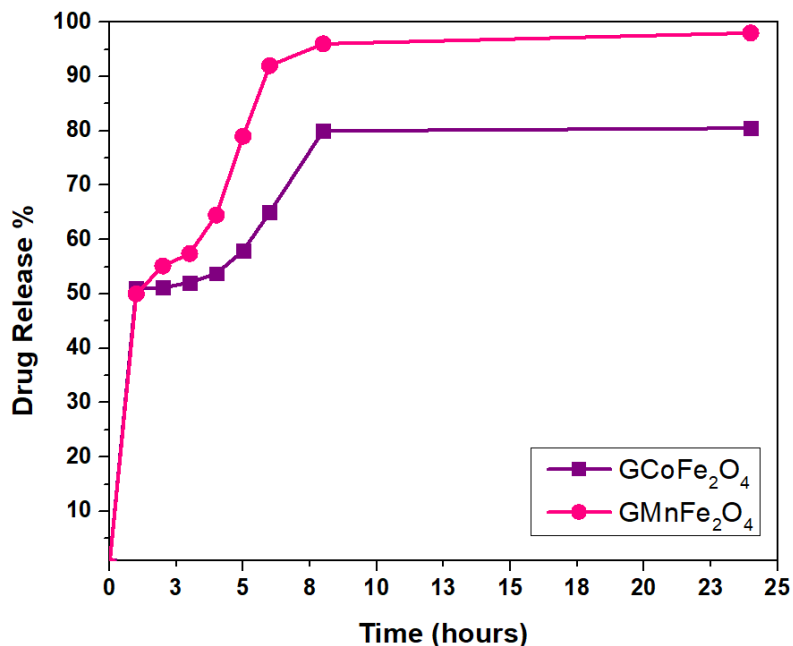


Figure 5.7: Drug release study of Gelatin coated, drug loaded CoFe₂O₄ and MnFe₂O₄ Nanocomposites

In this study, we conducted drug release tests on two gelatin-coated samples, G-CoFe₂O₄ and G-MnFe₂O₄, both containing the drug ciprofloxacin. The drug release was measured over time using UV spectroscopy. The graph depicts the percentage of drug

released from the samples at different time intervals, revealing distinct drug release profiles for the two materials.

Table 5.3: Comparison of drug release rates from G-CoFe₂O₄ and G-MnFe₂O₄

Features	G-CoFe ₂ O ₄	G-MnFe ₂ O ₄
Total amount of drug released	90%	80%
Drug release rate	Faster	Slower
Porosity	More porous	Less porous

The drug release percentage at a given time (t) was calculated using the following formula[96]:

$$(\text{Drug release percentage at time}) t = \frac{(\text{Absorbance of sample at time}(t) - (\text{Absorbance of sample at 0 hour}))}{(\text{Initial concentration of drug})} \times 100$$

The results demonstrate that G-CoFe₂O₄ releases a greater amount of drug compared to G- MnFe₂O₄. This difference in drug release can be attributed to the distinct properties of the two materials. G-CoFe₂O₄, being more porous, facilitates a higher drug release due to increased drug diffusion. [97]

The drug release behavior of both materials reached a plateau in the graph, indicating a diffusion-controlled release mechanism. This suggests that the rate of drug release is limited by the rate at which the drug can diffuse out of the samples.[98] The drug release test was conducted in phosphate-buffered saline (PBS) at 37°C for 24 hours, adhering to standard conditions for such studies.[94]

Overall, these findings imply that G-CoFe₂O₄ holds promise as a superior drug delivery system compared to G-MnFe₂O₄. The higher drug release and faster release rate exhibited by G- CoFe₂O₄ suggest its potential in achieving better therapeutic outcomes. This study sheds light on the importance of material properties in drug delivery systems

and underscores the significance of selecting suitable materials to optimize drug release kinetics for enhanced efficacy in medical applications.[93]

5.6.3 Higuchi Model Perspectives on Drug Release Diversity

The Higuchi model's applicability in deciphering drug release mechanisms was explored in this study. The model is employed as:

$$Q(t) = KH\sqrt{t}$$

where $Q(t)$ is the cumulative percentage of drug released at time t KH is the Higuchi constant t is the time The Higuchi constant, KH , can be obtained from the slope of the linear regression line[99]. For G-CoFe₂O₄ samples, the model fitted well, aligning data points linearly. The linear regression yielded a slope of 0.098, consistent with the anticipated diffusion-controlled release mechanism [100].

The diffusion-controlled release mechanism characterizes drug release from a polymer matrix via molecular diffusion towards the surface, followed by release into the surrounding medium. This mechanism depends on factors such as the diffusion coefficient within the polymer matrix and its thickness. The Higuchi model, an extension of the diffusion-controlled release mechanism, considers the polymer matrix's swelling. Here, drug molecules traverse a hydrated surface layer atop the polymer matrix. This model incorporates parameters like the diffusion coefficient within the hydrated layer and its thickness to determine the drug release rate[97].

The strong alignment between G-CoFe₂O₄ data and the linear model highlights the Higuchi model's suitability. This model suggests drug release guided by diffusion through a hydrated layer, further supported by the linear regression's slope of 0.098, affirming the diffusion-controlled release mechanism.

In contrast, G-MnFe₂O₄ data showed weak alignment with the linear line, indicating the Higuchi model's inadequacy. This suggests a distinct drug release mechanism, differing from diffusion through a hydrated layer. Evidently, the drug release mechanism for G-MnFe₂O₄ samples may differ from G-CoFe₂O₄ samples.

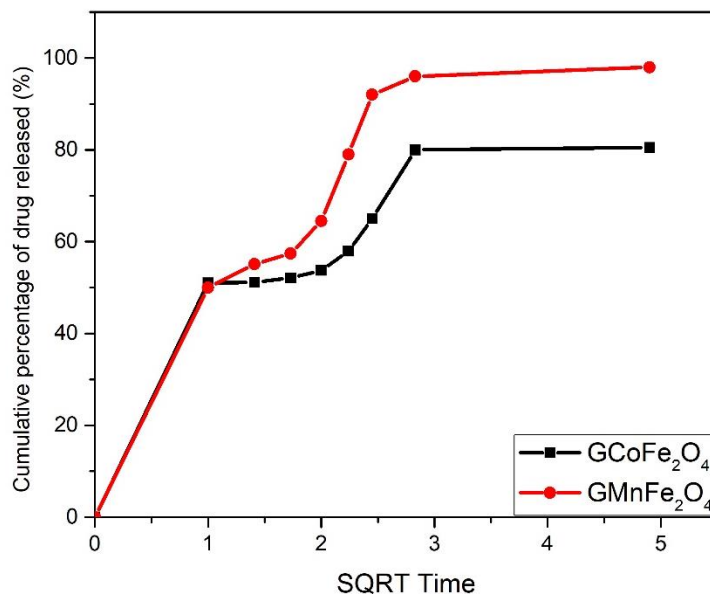


Figure 5.8: Cumulative percentage of drug released from G-CoFe₂O₄ and G-MnFe₂O₄ samples versus the square root of time.

In summary, the investigation revealed G-CoFe₂O₄ samples' adherence to the Higuchi model, implying diffusion-controlled drug release. This trait is crucial for precise drug delivery, ensuring controlled release rates.

These findings shed light on drug release dynamics for both G-CoFe₂O₄ and G-MnFe₂O₄. Further research is needed to unveil G-MnFe₂O₄'s specific drug release mechanism, enhancing understanding of these materials' attributes and potential in drug delivery applications.

CHAPTER 7: CONCLUSIONS AND FUTURE RECOMMENDATION

7.1 Conclusion

In this study, we synthesized gelatin-coated cobalt ferrite and manganese ferrite nanoparticles using a biocompatible polymer. The synthesis and characterization of gelatin-coated cobalt and manganese ferrite nanoparticles have provided valuable insights into their potential applications in drug delivery systems. The study demonstrated that the gelatin coating has a significant impact on the structural and magnetic properties of the nanoparticles, making them promising candidates for biomedical applications. The gelatin coating influenced particle growth while maintaining crystal structure integrity, underscoring its role in preserving material functionality. The nanoparticles exhibited distinct magnetic behaviors: gelatin-coated cobalt ferrite displayed high coercivity for targeted delivery, while gelatin-coated manganese ferrite showed potential for controlled release upon magnetic field exposure. Moreover, the study identified specific Raman modes for precise drug release control. These findings offer a foundation for optimizing drug delivery systems using these nanoparticles. Future research should focus on understanding the specific drug release mechanism of gelatin-coated manganese ferrite, exploring interactions with diverse drugs, assessing biocompatibility, and ensuring long-term stability for clinical applications.

7.2 Future Recommendations

Future research should focus further on the possible uses of gelatin-coated cobalt ferrite and manganese ferrite nanoparticles in drug delivery systems, building on the knowledge obtained from this work. A thorough analysis of the drug release mechanism of gelatin-coated manganese ferrite nanoparticles is a crucial area for inquiry. Optimising the use of these nanoparticles in targeted therapeutics requires a mechanistic understanding of how they release medications in response to magnetic fields. In order to determine these nanoparticles' adaptability and compatibility with different pharmacological chemicals, it is also important to investigate how they interact with a wider spectrum of medications. In-

depth biocompatibility studies are furthermore necessary to guarantee the security and effectiveness of these nanoparticles in biomedical applications.

Validating their fitness for clinical application will need long-term stability tests under physiological circumstances. We can progress the design and optimization of gelatin-coated cobalt and manganese ferrite nanoparticle-based drug delivery systems, possibly revolutionizing the area of targeted drug administration, by tackling these important research topics.

REFERENCES

- [1] S. Amiri, H. J. M. S. Shokrollahi, and E. C, "The role of cobalt ferrite magnetic nanoparticles in medical science," vol. 33, no. 1, pp. 1-8, 2013.
- [2] M. Wu and A. Hoffmann, "Recent advances in magnetic insulators-from spintronics to microwave applications," 2013.
- [3] L. Wang, L. Zhuo, H. Cheng, C. Zhang, and F. J. J. o. P. S. Zhao, "Porous carbon nanotubes decorated with nanosized cobalt ferrite as anode materials for high-performance lithium-ion batteries," vol. 283, pp. 289-299, 2015.
- [4] B. Issa, I. M. Obaidat, B. A. Albiss, and Y. J. I. j. o. m. s. Haik, "Magnetic nanoparticles: surface effects and properties related to biomedicine applications," vol. 14, no. 11, pp. 21266-21305, 2013.
- [5] S. Ammar *et al.*, "Magnetic properties of ultrafine cobalt ferrite particles synthesized by hydrolysis in a polyol mediumBasis of a presentation given at Materials Discussion No. 3, 26–29 September, 2000, University of Cambridge, UK," vol. 11, no. 1, pp. 186-192, 2001.
- [6] N. P. Ngema, "Synthesis, structural and magnetic properties of $\text{Co}_x\text{Fe}_{2-x}\text{O}_4$ and $\text{M}_0\text{Ni}_0\text{Fe}_2\text{O}_4$ ($\text{M} = \text{Mg, Ca, Sr, Ba}$) nanoferrites," 2017.
- [7] D. J. Griffiths, "Introduction to electrodynamics," ed: American Association of Physics Teachers, 2005.
- [8] L. Ajroudi, S. Villain, V. Madigou, N. Mliki, and C. J. J. o. C. G. Leroux, "Synthesis and microstructure of cobalt ferrite nanoparticles," vol. 312, no. 16-17, pp. 2465-2471, 2010.
- [9] Y. Zhang *et al.*, "Composition and magnetic properties of cobalt ferrite nanoparticles prepared by the co-precipitation method," vol. 322, no. 21, pp. 3470-3475, 2010.
- [10] B. M. Moskowitz, "Hitchhiker's guide to magnetism," in *Environmental Magnetism Workshop (IRM)*, 1991, vol. 279, no. 1, p. 48: Inst. for Rock Magnetism Univ. of Minn., Minneapolis, Minn.
- [11] S. Kyeong *et al.*, "Magnetic nanoparticles," pp. 191-215, 2021.
- [12] J. Zhang, W. Kosaka, Y. Kitagawa, and H. J. N. C. Miyasaka, "A metal–organic framework that exhibits CO₂-induced transitions between paramagnetism and ferrimagnetism," vol. 13, no. 2, pp. 191-199, 2021.

- [13] M. Mumtaz, M. Hassan, S. Ullah, and Z. J. C. Ahmad, "Nanohybrids of multi-walled carbon nanotubes and cobalt ferrite nanoparticles: High performance anode material for lithium-ion batteries," vol. 171, pp. 179-187, 2021.
- [14] S. Arcaro, J. Venturini, S. Arcaro, J. J. M. F. i. E. S. Venturini, Processing, and C.-E. Applications, "A Brief History of Ferrites," pp. 1-4, 2021.
- [15] J. Sánchez-Martín *et al.*, "High-Pressure X-ray Diffraction and DFT Studies on Spinel FeV₂O₄," vol. 13, no. 1, p. 53, 2022.
- [16] W. Zhang *et al.*, "Structural and magnetic properties of Ni–Cu–Co ferrites prepared from sol-gel auto combustion method with different complexing agents," vol. 816, p. 152501, 2020.
- [17] J. J. E. Coey, "Perspective and prospects for rare earth permanent magnets," vol. 6, no. 2, pp. 119-131, 2020.
- [18] C. de Julian Fernandez, C. Sangregorio, J. De La Figuera, B. Belec, D. Makovec, and A. J. J. o. P. D. A. P. Quesada, "Progress and prospects of hard hexaferrites for permanent magnet applications," vol. 54, no. 15, p. 153001, 2021.
- [19] S. B. Narang, K. J. J. o. M. Pubby, and M. Materials, "Nickel spinel ferrites: a review," vol. 519, p. 167163, 2021.
- [20] L. N. Warr and G. H. Grathoff, "Geoscientific Applications of Particle Detection and Imaging Techniques with Special Focus on Monitoring Clay Mineral Reactions," in *Handbook of Particle Detection and Imaging*: Springer, 2021, pp. 945-962.
- [21] S. C. Tolani, A. Golhar, and K. Rewatkar, "A review of morphological, structural behaviour and technological applications of ferrites," in *AIP Conference Proceedings*, 2019, vol. 2104, no. 1, p. 030032: AIP Publishing LLC.
- [22] V. V. Jadhav, R. S. Mane, P. V. Shinde, V. V. Jadhav, R. S. Mane, and P. V. J. B.-F.-B. E. S. Shinde, "Basics of Ferrites: Structures and Properties," pp. 37-45, 2020.
- [23] I. Unit, "Orthogonality. Laguerre functions: Laguerre and associated Laguerre polynomials, recursion relations; Orthogonality. Applications of special functions to problems in physics."
- [24] P. Dhiman, R. Jasrotia, D. Goyal, G. T. J. F. N. w. T. P. Mola, and D. Applications, "Hexagonal Ferrites, Synthesis, Properties and Their Applications," vol. 112, p. 336, 2021.
- [25] N. Kumari, S. Kour, G. Singh, and R. K. Sharma, "A brief review on synthesis, properties and applications of ferrites," in *AIP Conference Proceedings*, 2020, vol. 2220, no. 1, p. 020164: AIP Publishing LLC.

- [26] S. B. Shelke, *Studies on the Structural, Electrical and Magnetic Properties of Some Substituted Spinel Ferrites*. Insta Publishing, 2020.
- [27] E. Pervaiz, I. J. J. o. m. Gul, and m. materials, "High frequency AC response, DC resistivity and magnetic studies of holmium substituted Ni-ferrite: A novel electromagnetic material," vol. 349, pp. 27-34, 2014.
- [28] F. Hirosawa and T. J. S. S. S. Iwasaki, "A comparative study of the magnetic induction heating properties of rare earth (RE= Y, La, Ce, Pr, Nd, Gd and Yb)-substituted magnesium–zinc ferrites," vol. 118, p. 106655, 2021.
- [29] R. C. J. P. i. M. S. Pullar, "Hexagonal ferrites: a review of the synthesis, properties and applications of hexaferrite ceramics," vol. 57, no. 7, pp. 1191-1334, 2012.
- [30] D. Narsimulu, O. Padmaraj, E. Srinadhu, and N. J. J. o. M. S. M. i. E. Satyanarayana, "Synthesis, characterization and electrical properties of mesoporous nanocrystalline CoFe_2O_4 as a negative electrode material for lithium battery applications," vol. 28, pp. 17208-17214, 2017.
- [31] M. Rahimi-Nasrabadi, M. Rostami, F. Ahmadi, A. F. Shojaie, and M. D. J. J. o. M. S. M. i. E. Rafiee, "Synthesis and characterization of $\text{ZnFe}_{2-x}\text{Yb}_x\text{O}_4$ –graphene nanocomposites by sol–gel method," vol. 27, pp. 11940-11945, 2016.
- [32] X. Wang *et al.*, "Low temperature synthesis of metastable lithium ferrite: magnetic and electrochemical properties," vol. 16, no. 11, p. 2677, 2005.
- [33] V. Rathod, A. Anupama, V. Jali, V. Hiremath, and B. J. C. I. Sahoo, "Combustion synthesis, structure and magnetic properties of Li-Zn ferrite ceramic powders," vol. 43, no. 16, pp. 14431-14440, 2017.
- [34] E. Casbeer, V. K. Sharma, X.-Z. J. S. Li, and P. Technology, "Synthesis and photocatalytic activity of ferrites under visible light: a review," vol. 87, pp. 1-14, 2012.
- [35] M. J. J. o. A. Kaiser and Compounds, "Effect of nickel substitutions on some properties of Cu–Zn ferrites," vol. 468, no. 1-2, pp. 15-21, 2009.
- [36] S. Kumbhar *et al.*, "Structural, dielectric and magnetic properties of Ni substituted zinc ferrite," vol. 363, pp. 114-120, 2014.
- [37] M. Z. Khan, I. H. Gul, M. M. Baig, A. N. J. J. o. A. Khan, and Compounds, "Comprehensive study on structural, electrical, magnetic and photocatalytic degradation properties of Al^{3+} ions substituted nickel ferrites nanoparticles," vol. 848, p. 155795, 2020.
- [38] F. Finetti, E. Terzuoli, S. Donnini, M. Uva, M. Ziche, and L. J. P. o. Morbidelli, "Monitoring endothelial and tissue responses to cobalt ferrite nanoparticles and hybrid hydrogels," vol. 11, no. 12, p. e0168727, 2016.

- [39] J. Parhizkar, M. H. Habibi, and S. Y. J. S. Mosavian, "Synthesis and characterization of nano CoFe_2O_4 prepared by sol-gel auto-combustion with ultrasonic irradiation and evaluation of photocatalytic removal and degradation kinetic of reactive red 195," vol. 11, pp. 1119-1129, 2019.
- [40] B. Sahoo *et al.*, "Biocompatible mesoporous silica-coated superparamagnetic manganese ferrite nanoparticles for targeted drug delivery and MR imaging applications," vol. 431, pp. 31-41, 2014.
- [41] N. Akhlaghi, G. J. J. o. I. Najafpour-Darzi, and E. Chemistry, "Manganese ferrite (MnFe_2O_4) Nanoparticles: From synthesis to application-A review," vol. 103, pp. 292-304, 2021.
- [42] S. Ayyanaar *et al.*, "ROS-responsive chitosan coated magnetic iron oxide nanoparticles as potential vehicles for targeted drug delivery in cancer therapy," pp. 3333-3346, 2020.
- [43] S. Majeed *et al.*, "Bacteria mediated synthesis of iron oxide nanoparticles and their antibacterial, antioxidant, cytocompatibility properties," vol. 32, pp. 1083-1094, 2021.
- [44] G. Wang *et al.*, "Controlled synthesis of L-cysteine coated cobalt ferrite nanoparticles for drug delivery," vol. 44, no. 12, pp. 13588-13594, 2018.
- [45] G. A. Rather *et al.*, "The role of green synthesised zinc oxide nanoparticles in agriculture," pp. 119-142, 2022.
- [46] S. Keshri and S. J. P. i. B. Biswas, "Synthesis, physical properties, and biomedical applications of magnetic nanoparticles: a review," vol. 11, no. 4, pp. 347-372, 2022.
- [47] B. Dumontel, V. Conejo-Rodríguez, M. Vallet-Regí, and M. J. P. Manzano, "Natural Biopolymers as Smart Coating Materials of Mesoporous Silica Nanoparticles for Drug Delivery," vol. 15, no. 2, p. 447, 2023.
- [48] S. Gul *et al.*, "Al-substituted zinc spinel ferrite nanoparticles: preparation and evaluation of structural, electrical, magnetic and photocatalytic properties," vol. 46, no. 9, pp. 14195-14205, 2020.
- [49] B. Das *et al.*, "Chemically induced magnetic dead shells in superparamagnetic ni nanoparticles deduced from polarized small-angle neutron scattering," vol. 14, no. 29, pp. 33491-33504, 2022.
- [50] K. Shahzadi *et al.*, "Impact of aluminum substitution on the structural and dielectric properties of Ni-Cu spinel ferrite nanoparticles synthesized via sol-gel route," vol. 52, pp. 1-17, 2020.

- [51] D. Ravinder, G. R. Mohan, and D. J. M. L. Sagar, "High frequency dielectric behaviour of aluminium-substituted lithium ferrites," vol. 44, no. 3-4, pp. 256-260, 2000.
- [52] M. Rahman, N. Hasan, M. Hoque, M. Hossen, and M. J. R. i. P. Arifuzzaman, "Structural, dielectric, and electrical transport properties of Al³⁺ substituted nanocrystalline Ni-Cu spinel ferrites prepared through the sol-gel route," vol. 38, p. 105610, 2022.
- [53] S. Kumar, P. Bhushan, S. J. E. Bhattacharya, chemical, and m. sensors, "Fabrication of nanostructures with bottom-up approach and their utility in diagnostics, therapeutics, and others," pp. 167-198, 2018.
- [54] V. Arole and S. J. J. M. S. Munde, "Fabrication of nanomaterials by top-down and bottom-up approaches-an overview," vol. 1, pp. 89-93, 2014.
- [55] S. Hamatani, D. Kitagawa, R. Maegawa, and S. J. M. A. Kobatake, "Photochromic behavior of diarylbenzene nanoparticles prepared by top-down and bottom-up approaches," vol. 3, no. 2, pp. 1280-1285, 2022.
- [56] P. Pattekari, Z. Zheng, X. Zhang, T. Levchenko, V. Torchilin, and Y. J. P. C. C. P. Lvov, "Top-down and bottom-up approaches in production of aqueous nanocolloids of low solubility drug paclitaxel," vol. 13, no. 19, pp. 9014-9019, 2011.
- [57] A. E. Danks, S. R. Hall, and Z. J. M. H. Schnepf, "The evolution of 'sol-gel' chemistry as a technique for materials synthesis," vol. 3, no. 2, pp. 91-112, 2016.
- [58] S. B. Somvanshi, M. V. Khedkar, P. B. Kharat, and K. J. C. I. Jadhav, "Influential diamagnetic magnesium (Mg²⁺) ion substitution in nano-spinel zinc ferrite (ZnFe₂O₄): thermal, structural, spectral, optical and physisorption analysis," vol. 46, no. 7, pp. 8640-8650, 2020.
- [59] M. E. Taygun and A. Boccaccini, "Nanoscaled bioactive glass particles and nanofibers," in *Bioactive Glasses*: Elsevier, 2018, pp. 235-283.
- [60] G. Tartaro, H. Mateos, D. Schirone, R. Angelico, and G. J. N. Palazzo, "Microemulsion microstructure (s): A tutorial review," vol. 10, no. 9, p. 1657, 2020.
- [61] T. Tatarchuk, M. Bououdina, J. Judith Vijaya, and L. John Kennedy, "Spinel ferrite nanoparticles: synthesis, crystal structure, properties, and perspective applications," in *Nanophysics, Nanomaterials, Interface Studies, and Applications: Selected Proceedings of the 4th International Conference Nanotechnology and Nanomaterials (NANO2016), August 24-27, 2016, Lviv, Ukraine, 2017*, pp. 305-325: Springer.

- [62] O. F. Odio, E. J. M. s.-s. Reguera, properties, and applications, "Nanostructured spinel ferrites: Synthesis, functionalization, nanomagnetism and environmental applications," pp. 185-216, 2017.
- [63] K. K. Kefeni and B. B. J. J. o. C. P. Mamba, "Evaluation of charcoal ash nanoparticles pollutant removal capacity from acid mine drainage rich in iron and sulfate," vol. 251, p. 119720, 2020.
- [64] R. Wu, J. Qu, H. He, and Y. J. A. C. B. E. Yu, "Removal of azo-dye Acid Red B (ARB) by adsorption and catalytic combustion using magnetic CuFe_2O_4 powder," vol. 48, no. 1, pp. 49-56, 2004.
- [65] W. S. Saad and R. K. J. N. T. Prud'homme, "Principles of nanoparticle formation by flash nanoprecipitation," vol. 11, no. 2, pp. 212-227, 2016.
- [66] N. Dudchenko, S. Pawar, I. Perelshtein, and D. J. M. Fixler, "Magnetite nanoparticles: synthesis and applications in optics and nanophotonics," vol. 15, no. 7, p. 2601, 2022.
- [67] A. A. Bunaciu, E. G. UdrişTioiu, and H. Y. J. C. r. i. a. c. Aboul-Enein, "X-ray diffraction: instrumentation and applications," vol. 45, no. 4, pp. 289-299, 2015.
- [68] A. A. Chernov, *Modern crystallography III: crystal growth*. Springer Science & Business Media, 2012.
- [69] I. Gul, A. Abbasi, F. Amin, M. Anis-ur-Rehman, A. J. J. o. m. Maqsood, and m. materials, "Structural, magnetic and electrical properties of $\text{Co}_{1-x}\text{Zn}_x\text{Fe}_2\text{O}_4$ synthesized by co-precipitation method," vol. 311, no. 2, pp. 494-499, 2007.
- [70] M. Tare, O. R. Puli, S. M. Oros, and A. J. D. I. S. Singh, "Drosophila adult eye model to teach Scanning Electron Microscopy in an undergraduate cell biology laboratory," vol. 92, 2009.
- [71] C. Berthomieu and R. J. P. r. Hienerwadel, "Fourier transform infrared (FTIR) spectroscopy," vol. 101, pp. 157-170, 2009.
- [72] D.-W. Sun, *Infrared spectroscopy for food quality analysis and control*. Academic press, 2009.
- [73] S. Naghash-Hamed, N. Arsalani, and S. B. J. N. F. Mousavi, "Facile copper ferrite/carbon quantum dot magnetic nanocomposite as an effective nanocatalyst for reduction of para-nitroaniline and ortho-nitroaniline," vol. 6, no. 4, p. 045003, 2022.
- [74] D. Balatskiy, Y. Budnikova, S. Bratskaya, and M. J. J. o. C. S. Vasilyeva, " TiO_2 - CoFe_2O_4 and TiO_2 - CuFe_2O_4 Composite Films: A New Approach to Synthesis, Characterization, and Optical and Photocatalytic Properties," vol. 7, no. 7, p. 295, 2023.

- [75] F. Mushtaq *et al.*, "Preparation, properties, and applications of gelatin-based hydrogels (GHs) in the environmental, technological, and biomedical sectors," 2022.
- [76] G. Battogtokh, Y. Joo, S. M. Abuzar, H. Park, and S.-J. J. M. Hwang, "Gelatin coating for the improvement of stability and cell uptake of hydrophobic drug-containing liposomes," vol. 27, no. 3, p. 1041, 2022.
- [77] S. Z. H. Hashmi *et al.*, "Synthesis of Nickel-doped Magnesium spinel ferrites ($\text{Ni}_x\text{Mg}_{1-x}\text{Fe}_2\text{O}_4$) nanomaterials and study of their structural, electrical and magnetic properties," vol. 305, p. 127912, 2023.
- [78] K. Dixit *et al.*, "Gum tragacanth modified nano-hydroxyapatite: An angiogenic-osteogenic biomaterial for bone tissue engineering," vol. 48, no. 10, pp. 14672-14683, 2022.
- [79] P. Ma *et al.*, "Recent advances in mechanical force-responsive drug delivery systems," vol. 4, no. 17, pp. 3462-3478, 2022.
- [80] N. Parikh and K. J. J. o. M. S. M. i. M. Parekh, "Technique to optimize magnetic response of gelatin coated magnetic nanoparticles," vol. 26, no. 7, p. 202, 2015.
- [81] I. A. Parray, A. Somvanshi, and S. A. J. C. I. Ali, "Study of microstructural, ferroelectric and magnetic properties of cerium substituted magnesium ferrite and its potential application as hydroelectric cell," vol. 49, no. 4, pp. 6946-6957, 2023.
- [82] M. Junaid *et al.*, "Structural, microstructural, spectral, and dielectric properties of erbium substituted spinel ferrites," vol. 641, p. 414120, 2022.
- [83] L. V. Hublikar, S. V. Ganachari, V. B. J. E. S. Patil, and P. Research, "Zn and Co ferrite nanoparticles: towards the applications of sensing and adsorption studies," vol. 30, no. 25, pp. 66994-67007, 2023.
- [84] J. Liu, R. Chen, J. Yang, Y. Li, and D. J. J. o. C. H. Hu, "Historical photo curling and fracture mainly caused by the surface performance change of gelatin resulting from alternating dry-wet environment," vol. 61, pp. 57-64, 2023.
- [85] A. Bahoor, R. Ahmadi, M. Heydari, M. Bagheri, and A. J. I. C. C. Behnamghader, "Synthesis and evaluation of cross-linked gelatin nanoparticles for controlled release of an anti-diabetic drug: Gliclazide," vol. 154, p. 110856, 2023.
- [86] D. Gingasu *et al.*, "Synthesis of CoFe_2O_4 through Wet Ferritization Method Using an Aqueous Extract of Eucalyptus Leaves," vol. 13, no. 7, p. 1250, 2023.
- [87] S. Carregal-Romero *et al.*, "Ultrasmall manganese ferrites for in vivo catalase mimicking activity and multimodal bioimaging," vol. 18, no. 16, p. 2106570, 2022.

- [88] J. R. D. Santos *et al.*, "Nanoparticles of Mixed-Valence Oxides $MnXCO_3-XO_4$ ($0 \leq X \leq 1$) Obtained with Agar-Agar from Red Algae (Rhodophyta) for Oxygen Evolution Reaction," vol. 12, no. 18, p. 3170, 2022.
- [89] F. Mohammadi *et al.*, "The potential of surface nano-engineering in characteristics of cobalt-based nanoparticles and biointerface interaction with prokaryotic and human cells," vol. 215, p. 112485, 2022.
- [90] A. Nahar, "Synthesis and Magnetic Properties of Folate Chitosan Coated Cobalt Ferrite Nanoparticles for Biomedical Applications," © University of Dhaka, 2022.
- [91] M. B. Islam, M. R. Pavel, M. R. Islam, and M. J. J. J. o. E. S. Haque, "Synthesis of Cobalt Ferrite Nanoparticles Using Microemulsion Method: Structure, Morphology, and Magnetic Properties," vol. 13, no. 1, pp. 81-87, 2022.
- [92] D. Jose, S. Mildred, R. M. Sebastian, and S. Xavier, "An Investigative Study on the effect of Dopants on Manganese Based Mixed Nano Ferrites Synthesized through Sol-Gel Method," in *IOP Conference Series: Materials Science and Engineering*, 2022, vol. 1221, no. 1, p. 012036: IOP Publishing.
- [93] K. Ghosal, S. Chatterjee, S. Thomas, and P. J. A. P. Roy, "A detailed review on synthesis, functionalization, application, challenges, and current status of magnetic nanoparticles in the field of drug delivery and gene delivery system," vol. 24, no. 1, p. 25, 2022.
- [94] M. Poorhossein, F. Pishbin, A. Ataie, and M. J. C. I. Akrami, "Designing a multifunctional nanoplatform based on PEGylated cobalt ferrite magnetic nanoparticles containing capecitabine for cancer theranostics," vol. 49, no. 2, pp. 2705-2714, 2023.
- [95] V. Vinodhini and C. J. P. B. Krishnamoorthi, "Effect of dispersants on cytotoxic properties of magnetic nanoparticles: a review," vol. 79, no. 10, pp. 8143-8192, 2022.
- [96] T. Nalini, S. K. Basha, A. M. Sadiq, and V. S. J. M. T. C. Kumari, "Pectin/chitosan nanoparticle beads as potential carriers for quercetin release," vol. 33, p. 104172, 2022.
- [97] F. Vajhadin *et al.*, "Glutaraldehyde crosslinked doxorubicin promotes drug delivery efficiency using cobalt ferrite nanoparticles," vol. 220, p. 112870, 2022.
- [98] J. Gao *et al.*, "Hollow mesoporous structured $MnFe_2O_4$ nanospheres: A biocompatible drug delivery system with pH-responsive release for potential application in cancer treatment," vol. 135, p. 107066, 2023.
- [99] R. Mannu *et al.*, "Polyethylene glycol coated magnetic nanoparticles: Hybrid nanofluid formulation, properties and drug delivery prospects," vol. 11, no. 2, p. 440, 2021.

- [100] M. Z. Fahmi, R. A. Prasetya, M. F. Dzikri, S. C. W. Sakti, B. J. M. C. Yulianto, and Physics, "MnFe₂O₄ nanoparticles/cellulose acetate composite nanofiber for controllable release of naproxen," vol. 250, p. 123055, 2020.